The Astrophysical Journal, 596:1197–1219, 2003 October 20

AN EXTENSIVE CENSUS OF *HUBBLE SPACE TELESCOPE* COUNTERPARTS TO *CHANDRA* X-RAY SOURCES IN THE GLOBULAR CLUSTER 47 TUCANAE. II. TIME SERIES AND ANALYSIS[1]

Peter D. Edmonds,[2] Ronald L. Gilliland,[3] Craig O. Heinke,[2] and Jonathan E. Grindlay[2]

Received 2003 March 6; accepted 2003 June 30

ABSTRACT

We report time series and variability information for the optical identifications of X-ray sources in 47 Tucanae reported in Paper I (at least 22 cataclysmic variables [CVs] and 29 active binaries). The radial distribution of the CVs is indistinguishable from that of the millisecond pulsars (MSPs) detected by Freire et al. A study of the eight CVs with secure orbital periods (two obtained from the *Chandra* study of Grindlay et al.) shows that the 47 Tuc CVs have fainter accretion disks, in the V band, than field CVs with similar periods. These faint disks and the faint absolute magnitudes (M_V) of the 47 Tuc CVs suggests they have low accretion rates. One possible explanation is that the 47 Tuc objects may be a more representative sample of CVs, down to our detection threshold, than the CVs found in the field (where many low accretion rate systems are believed to be undiscovered), showing the advantages of deep globular cluster observations. The median F_X/F_{opt} value for the 47 Tuc CVs is higher than that of all known classes of field CV, partly because of the faint M_V values and partly because of the relatively high X-ray luminosities (L_X). The latter are only seen in DQ Her systems in the field, but the 47 Tuc CVs are much fainter optically than most field DQ Her's. Previous work by Edmonds et al. has shown that the four brightest CVs in NGC 6397 have optical spectra and broadband colors that are consistent with DQ Her's having lower than average accretion rates. Some combination of magnetic behavior and low accretion rates may be able to explain our observations, but the results at present are ambiguous, since no class of field CV has distributions of both L_X and M_V that are consistent with those of the 47 Tuc CVs.

The radial distribution of the X-ray detected active binaries is indistinguishable from that of the much larger sample of optical variables (eclipsing and contact binaries and BY Dra variables) detected in previous Wide Field Planetary Camera 2 (WFPC2) studies by Albrow et al. The X-ray properties of these objects (luminosity, hardness ratios, and variability) are consistent with those of active binaries found in field studies, and the F_X/F_{opt} distribution is significantly different from those of the CVs and the MSPs that are detected (or possibly detected) in the optical. Despite these results, we examine the possibility that a few of the active binaries are MSPs with main-sequence companions resulting from double exchanges in the crowded core of 47 Tuc. No solid evidence is found for a significant population of such objects, and therefore, using the methods of Grindlay et al., we estimate that the number of MSPs in 47 Tuc with luminosities above 10^{30} ergs s^{-1} is $\sim$30–40, near the previous lower limit. We present the results of a new, deeper search for faint low-mass X-ray binaries (LMXBs) in quiescence. One reasonable and one marginal candidate for optical identification of a quiescent LMXB was found (one is already known). Finally, it is shown that the periods of the blue variables showing little or no evidence for X-ray emission are too long for Roche lobe filling (if the variations are ellipsoidal). These blue variables also show no evidence for the large flickering levels seen in comparably bright CVs. At present we have no satisfactory explanation for these objects, although some may be detached white dwarf–main-sequence star binaries.

Subject headings: binaries: general — globular clusters: individual (47 Tucanae) — novae, cataclysmic variables — techniques: photometric — X-rays: binaries

1. INTRODUCTION

Binaries are well known to have a profound impact on the dynamical evolution of globular clusters (Hut et al. 1992; Edmonds et al. 2003, hereafter Paper I), and they offer an opportunity to study the results of stellar interactions. They also offer the crucial advantages of studying binary systems at the same, well-determined distance, age, metallicity, and reddening. Accurate distances are particularly important for reducing uncertainties in luminosities, and making reliable cluster-to-cluster comparisons and cluster-to-field comparisons.

Despite these promising goals, observational progress in detecting globular cluster binaries was initially slow, mainly because of spatial resolution and sensitivity limitations. However, the superb imaging capabilities of *Chandra* and the *Hubble Space Telescope* (*HST*) has now resulted in the detection of large numbers of compact binaries in several globular clusters (see Grindlay et al. 2001a, hereafter GHE01a, and references in Paper I). In particular, using the *Chandra* data of GHE01a and the *HST* data of Gilliland et al. (2000; *HST* program GO-8267), a large population of X-ray binaries with optical identifications has been found in 47 Tuc, with over 50 binaries reported in Paper I. There, the details of the astrometry and photometry for this sample

[1] Based on observations with the NASA/ESA *Hubble Space Telescope* obtained at STScI, which is operated by AURA, Inc. under NASA contract NAS 5-26555.

[2] Harvard-Smithsonian Center for Astrophysics, 60 Garden Street, Cambridge, MA 02138; pedmonds@cfa.harvard.edu, cheinke@cfa.harvard.edu, josh@cfa.harvard.edu.

[3] Space Telescope Science Institute, 3700 San Martin Drive, Baltimore, MD 21218; gillil@stsci.edu.

were reported, with most of the systems being identified as either accreting white dwarf–main-sequence star binaries (cataclysmic variables or CVs) or chromospherically "active binaries."

This paper reports *HST* optical time series and other detailed analysis for the sample of binaries reported in Paper I. Variability for most of the CVs is detected, confirming the CV identifications given in Paper I based on absolute photometry alone. In particular, flickering for the brighter optical IDs is found, plus periods for several of the higher inclination systems and some long-term variability. The CV periods and the absolute magnitudes determined in Paper I are compared with predictions for Roche lobe filling secondaries and are compared with CVs found in the field. Time series for the active binaries are also presented here, with an emphasis on the variables not discussed by Albrow et al. (2001; hereafter AGB01).

The radial distribution (radial offsets from cluster center) of the CVs and active binaries discovered in Paper I are compared with the radial distribution of MSPs from Freire et al. (2001) and with the total stellar population, to test whether these distributions are consistent with the expectations of mass segregation. Comparisons between the radial distributions of the X-ray detected active binaries and the larger sample of binaries discovered by AGB01 are also made.

Other important diagnostics examined here are the X-ray luminosities and optical magnitudes. The flux ratio between the two was shown by Richman (1996) and Verbunt et al. (1997; hereafter VBR97) to be inversely proportional to the CV accretion rate (for nonmagnetic systems), and here we make detailed comparisons between the 47 Tuc CVs and field CVs to help constrain the CV accretion rates in 47 Tuc. The X-ray to optical flux ratio is also useful in searching for additional quiescent low-mass X-ray binaries (qLMXBs) besides X5 and X7 (GHE01a and Heinke et al. 2003). We also discuss the X-ray luminosity and absolute magnitude distributions of the 47 Tuc CVs and compare to field systems.

The time series will be described in § 2, followed by an analysis section (§ 3), including a study of the radial distribution of the sources and their X-ray to optical flux ratios. This will be followed by a discussion in § 4, and an interpretation of the results given in both Papers I and II.

2. TIME SERIES

2.1. *Optical Data*

Paper I discusses the photometric results for the optical IDs (including the color-magnitude diagrams [CMDs]) in detail. Exquisite time series were produced in the V and I bands for the GO-8267 data set, and are analyzed in this paper. Detailed simulations were carried out by AGB01, giving the recovery rate of simulated variables as a function of period, V magnitude, and signal amplitude for the PC1 and WF2 chips. For amplitudes of Δ(intensity)/intensity $= 0.1$, the recovery rate for PC1 was $\sim$100% from the main-sequence turnoff (MSTO) to $V = 23.5$ for all input periods below 3.2 days, and for amplitudes of 0.01 the recovery rate fell from $\sim$70% at $V = 20$ to less than 10% at $V = 21.5$ (AGB01). The WF2 recovery rates extend to slightly fainter magnitudes (AGB01), but the generally higher crowding and saturation levels in the WF2 images counteract this gain, for variable searches.

2.2. *Cataclysmic Variables*

2.2.1. *GO-8267 Data*

For the CV candidates found in the GO-8267 field of view (FoV) (Paper I), we have analyzed the high-quality time series produced by the planet and binary searches of Gilliland et al. (2000) and AGB01. Time series were produced using difference image analysis combined with aperture and PSF-fitting photometry (see Gilliland et al. 2000 and AGB01 for more details). The size of the region used in the photometry extractions was decreased to as small as 1 pixel in the cases where plausible X-ray IDs were located near bright stars. Least-squares fits to sinusoids and the Lomb-Scargle periodogram were then applied to search for periodic variations in the time series of the CV candidates. Seven certain periodic variables were confirmed in this way: $W1_{opt}$, $W8_{opt}$, $W15_{opt}$, $W21_{opt}$, $W34_{opt}$, AKO 9, and the marginal ID for W71. We discuss each of these here in turn.

The ID for W1 is either a 2.89 hr or a 5.78 hr period variable (ellipsoidal variations). Examination of the light curves folded at the 2.89 and 5.78 hr periods, and of the power spectra, do not show unambiguous departures from sinusoidal light curves (Fig. 1), although the V-band phase plot does show some evidence for asymmetry at a little less than the 3 σ level, arguing for the longer period. We can use equation (2.102) from Warner (1995) to place limits on the absolute magnitude of the secondary:

$$M_V(2) = 16.7 - 11.1 \log P_{\rm orb}(h) \, , \qquad (1)$$

where $M_V(2)$ is the absolute magnitude of the secondary and $P_{\rm orb}$ is the orbital period measured in hours (where $2 \lesssim P_{\rm orb} \lesssim 10$ hr). This relationship is appropriate for field CVs of roughly solar metallicity. At fixed mass, stars with lower metallicity will have brighter secondaries (Stehle, Kolb, & Ritter 1997), and so equation (1) gives a lower limit to the luminosity of secondary stars in 47 Tuc (an upper limit to M_V). For $W1_{opt}$ ($M_V = 5.86$) using a 5.78 hr period gives a limit of $M_V = 8.2$ from equation (1), while using a

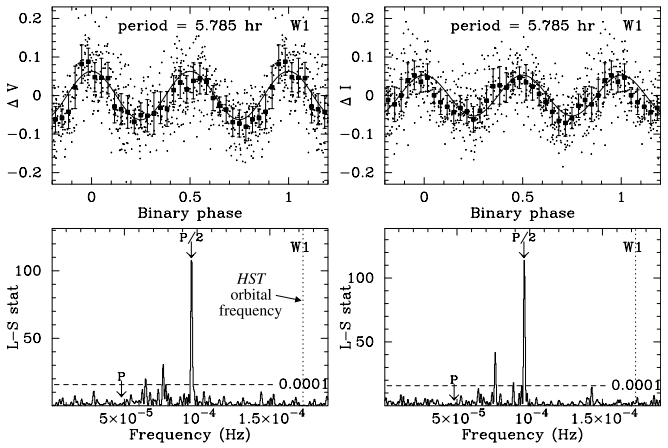

FIG. 1.—Phase plots and Lomb-Scargle power spectra in the V and I band for W1 (a CV). Individual points and phase bins (with 3 σ errors) are shown for the phase plots, and a sinusoid fit is overplotted. The orbital period (and half of it) are labeled on the power spectra, and the *HST* orbital frequency is shown. The horizontal dotted line shows the power level corresponding to a false-alarm probability of 1×10^{-4}.

2.89 hr period gives $M_V = 11.6$. The longer period is therefore favored unless the accretion disk completely dominates in the V band. This may be possible if W1 is a nonmagnetic nova-like CV, explaining the relatively blue $V-I$ color of $W1_{opt}$. However, the F_X/F_{opt} value for this system is much more consistent with a magnetic CV or a dwarf nova (DN) system (see Fig. 19 below), and a period of 2.89 hr would be shorter than any of the UX UMa systems given in Figure 10*a* (below), and all but one of the DQ Her systems. Modeling of the accretion disk and secondary in this system may help determine which period is correct.

Note that both $W8_{opt}$ and $W15_{opt}$ are optically crowded, and the absolute photometry in V and I is relatively poor (an I magnitude could not be self-consistently derived for $W15_{opt}$). However, since this project was optimized for time-series accuracy, the quality of the time series is much higher than that of the absolute photometry. Both $W8_{opt}$ and $W15_{opt}$ are clearly eclipsing systems (see Fig. 2), with unambiguous period determinations of 2.86 hr (at the upper edge of the period gap for field CVs) and 4.23 hr, respectively. Both of the associated X-ray sources for these CVs are very hard (GHE01a). Detection of these objects as eclipsing strongly supports the argument of GHE01a that self-absorption by the accretion disks are responsible for the hard spectra. See § 2.2.3 for more details about these two binaries.

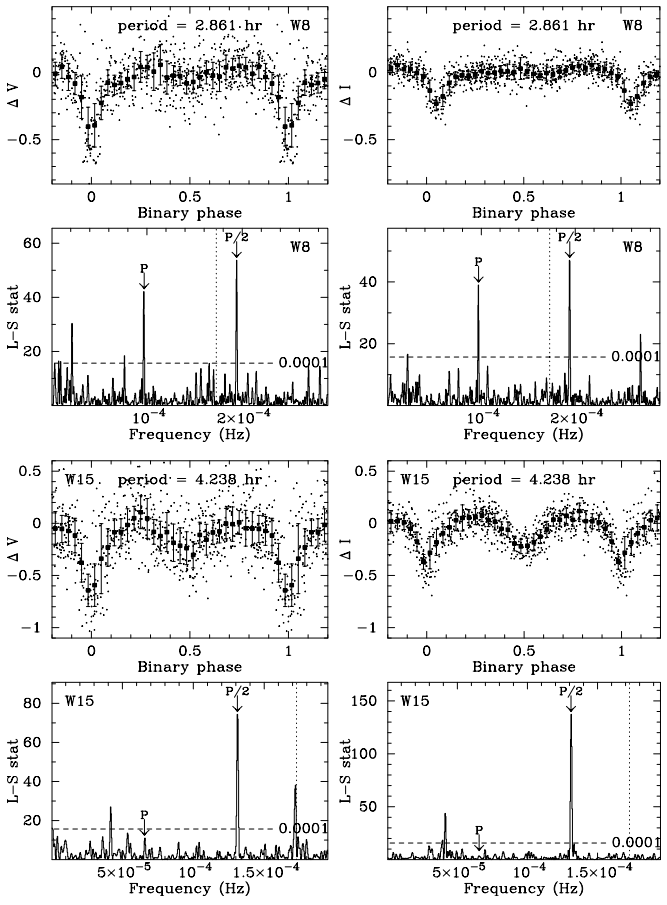

FIG. 2.—Phase plots and power spectra in the V and I band for the eclipsing CVs $W8_{opt}$ and $W15_{opt}$. Note, for both systems, the deeper eclipses in the V band compared to the I band because the blue accretion disk is being eclipsed. These CVs both have very hard X-ray spectra, likely caused by significant X-ray absorption by the accretion disk.

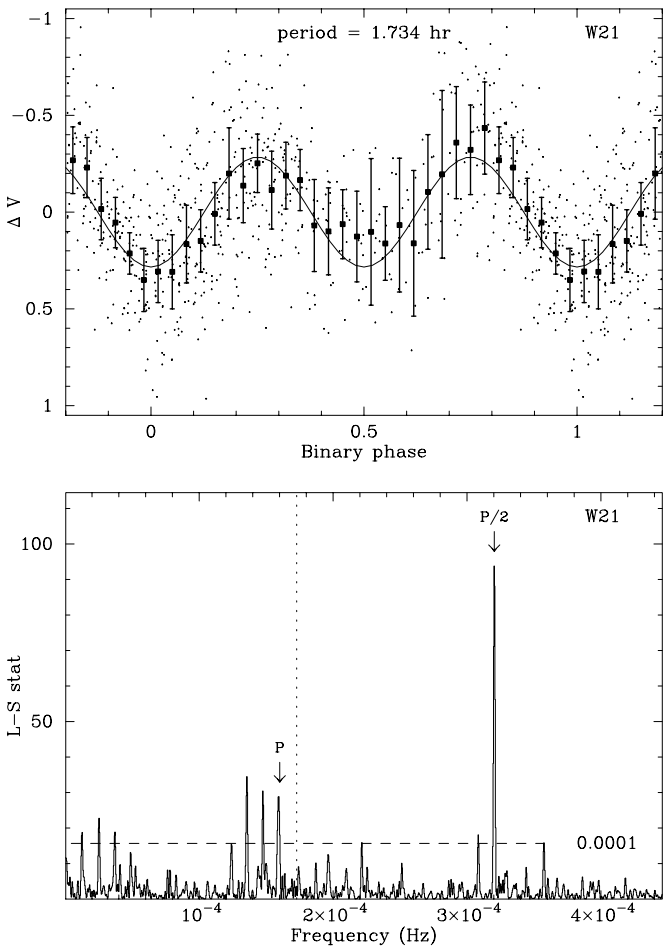

FIG. 3.—Phase plot and power spectrum in the V band for $W21_{opt}$, based on single–pixel photometry (because of saturation no useful data is available for I). We have assumed that the orbital period is 1.734 hr (for ellipsoidal variations), but the orbital period could also be 1.734/2 hr.

The ID for W21 is very near to a strong saturation trail, and evidence for a periodic signal was only detected in the single-pixel analysis. Figure 3 shows the secure 52 minute variation (this may also be a 104 minute orbital period). The lack of strong signal at 104 minutes in the power spectrum and the large amplitude of the time series (0.28 ± 0.14) tentatively favor 52 minutes being the orbital period. Poor phase coverage at phases 0.4–0.75 makes it difficult to distinguish between these two periods, although the phase plot does show suggestive evidence of asymmetry. In the 52 minute period case the secondary is possibly a degenerate star, since 52 minutes is well below the canonical period minimum for field CVs of $\sim$75 minutes, for nondegenerate secondaries. However, some field CVs with nondegenerate secondaries do have periods about this small (e.g., a 59 minute orbital period for V485 Cen; Augusteijn et al. 1996).

The light curve for $W34_{opt}$ is discussed in detail in Edmonds et al. (2002a). Although the strong 97.45 minute period is very close to the *HST* orbital period (96.5 minutes), Edmonds et al. (2002a) argue that this is not the result of an artifact showing up as a false signal at the *HST* orbit. The binary $W36_{opt}$ (AKO 9) is a long-period eclipsing CV with a subgiant secondary and a period unambiguously determined to be 1.108 days (see also Edmonds et al. 1996; GHE01a; Knigge et al. 2002a). The blue variable and possible counterpart to W71 has a 1.19 hr power spectrum signal with a likely

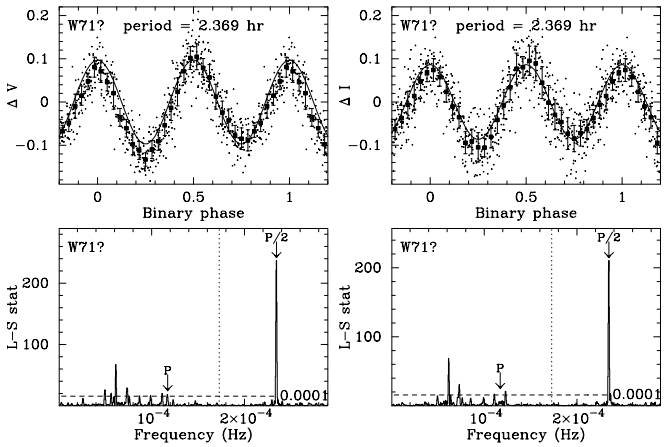

FIG. 4.—Phase plot and power spectrum for a blue variable and marginal optical counterpart to W71. There are small, but significant deviations of the phase plot from a sinusoidal curve (overlaid).

2.37 hr orbital period, based on the small but significant asymmetry in the phase plot using the longer period (see Fig. 4). If this is a CV, it would fall within the period gap for field CVs ($2.2 \lesssim P_{\rm orb} \lesssim 2.8$ hr). Although this variable may be a magnetic CV, and the source is relatively soft, consistent with an AM Her system, we favor the explanation (supported by the astrometry), that the *Chandra* source is not associated with the nearby blue, variable star (see § 3.4 for possible explanations of its nature).

For the other CV candidates, deeper searches for periodic variations were made and several marginal signals were found (see Fig. 5). For V1, the strongest *V*-band power spectrum peak in a reasonable period range corresponds to an orbital period of ~7 hr (for ellipsoidal variations). For V2, peaks are found at 13.67/2 hr (*V*) and 6.01/2 hr (*I*), and a strong signal is also seen in *V* at 1.44 days, and a 1.5 day signal in *I*. The shortest of these corresponds to a plausible

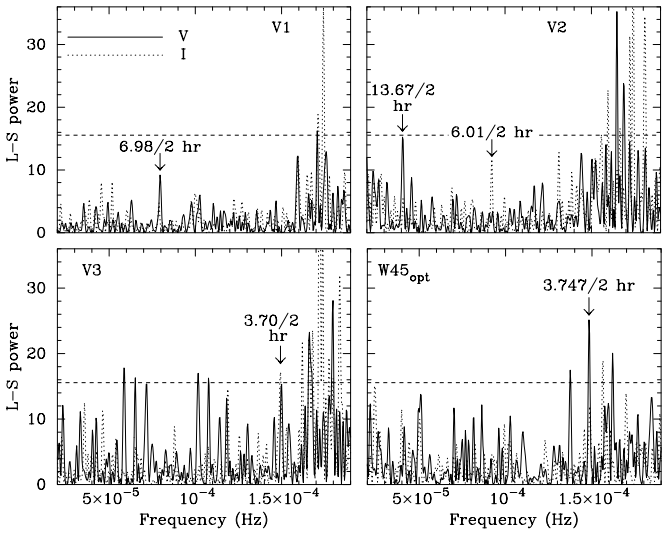

FIG. 5.—Power spectra in the *V* and *I* band for V1, V2, V3, and $W45_{opt}$. Possible periods are labeled (for ellipsoidal variations the periods will be twice the values shown). The X-ray counterpart to V3 (W27) has a period of 3.83 hr (GHE01a).

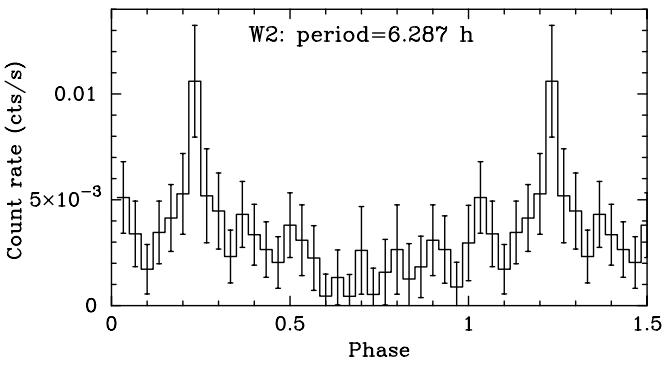

FIG. 6.—*Chandra* phase plot for W2 (a CV), folded at the period measured from the power spectrum, with 1 σ error bars.

orbital period, while the two longest ones are unlikely to be orbital periods for this apparent MS secondary, unless it is evolved. For V3, peaks are found in both *V* and *I* corresponding to a possible orbital period of ~3.7 hr (close to the 3.83 hr period present in the X-ray light curve; GHE01a). The ID for W45 shows a significant peak at 1.87 hr in *V* (possibly a 3.75 hr orbital period). A weaker signal is found in *I* at the same period and a strong signal at 1.78 hr.

The ID for W2 shows possible periods at 2.2, 5.9, and 8.2 hr. These differ from the statistically significant X-ray period of 6.287 hr (see Fig. 6 for an X-ray phase plot and Fig. 7*a* for a *V*-band power spectrum and phase plot). The power spectrum is extremely noisy, at least partly because the counterpart lies on a diffraction spike from a nearby giant star. Flickering may be an extra source of noise. The ID for W120 shows a marginally significant peak in the *V* power spectrum of 1.32 hr, with a false-alarm probability (FAP) of 1.4×10^{-2} (see Fig. 7*b*). The power spectrum is otherwise very clean, with no other peaks having a FAP < 0.9. The possible counterpart to W10 has a 2.2 or 4.4 hr period and may also be a CV, but crowding prevents us obtaining useful limits on the color.

Figure 8 shows plots of time-series rms versus *V* and *I* for the PC1, WF2, and WF4 chips (the few WF3 variables are shown on WF4). In the cases for which *I* values are not

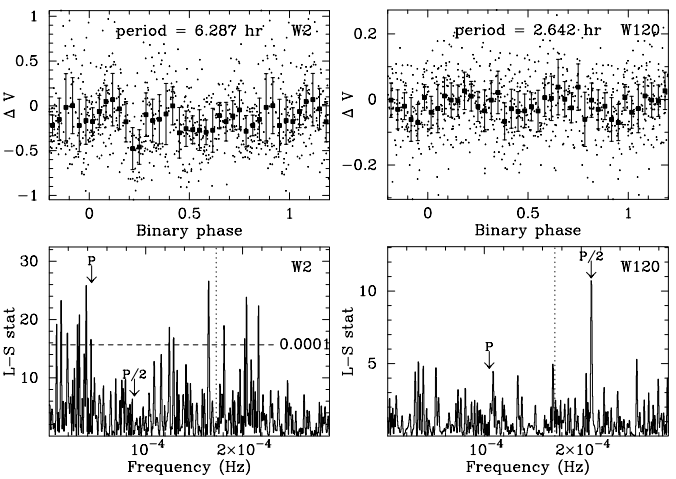

FIG. 7.—Phase plots and power spectra for the CVs $W2_{opt}$ and $W120_{opt}$. For $W2_{opt}$, the phase plot is folded at the X-ray period, and this period is labeled in the power spectrum.

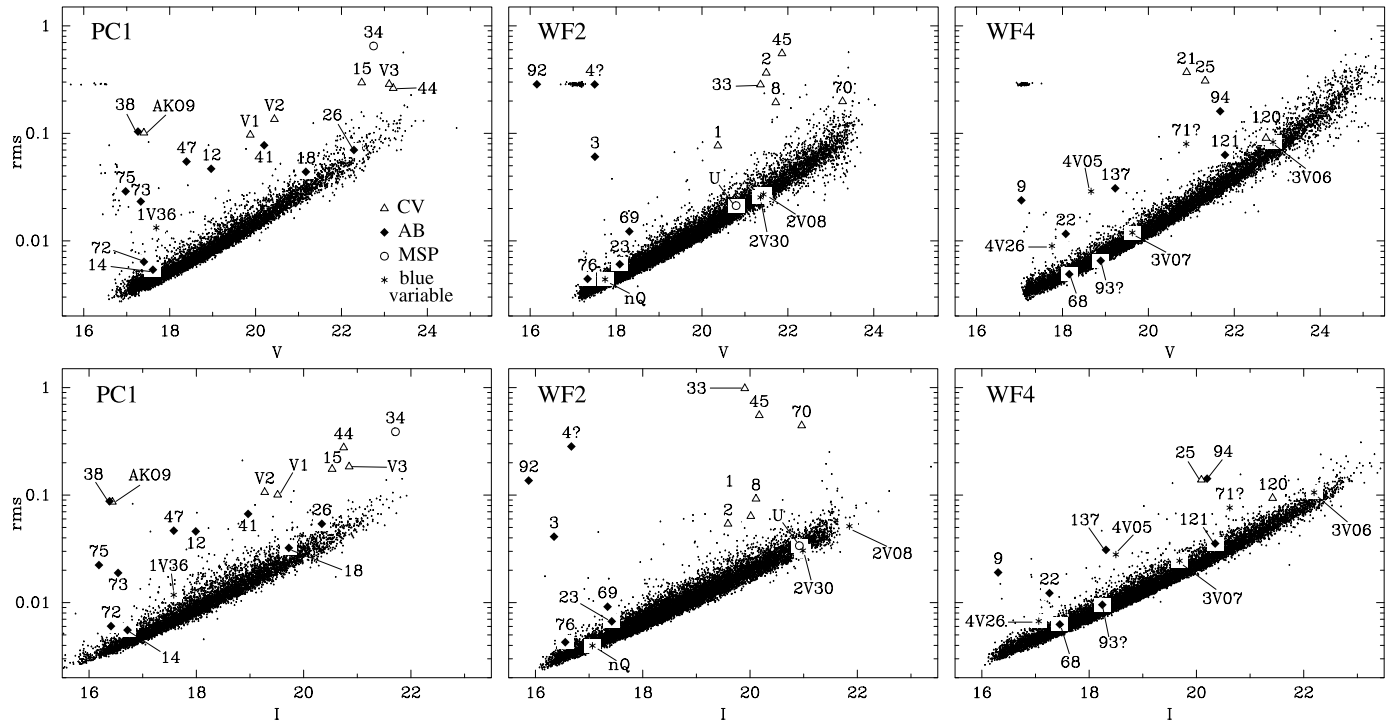

FIG. 8.—Plots of time series rms vs. V and I for optical counterparts to X-ray sources in the GO-8267 data, plus the blue variables discussed in § 3.4. The WF3 data (containing relatively few variables) is not shown, but 3V06 and 3V07 are included with the WF4 CMD. The clump of bright objects with rms values of ~0.3 are saturated stars in the V-band. The labeling shown in the PC1 plot for V is the same as that used in the CMDs of Paper I (*triangles*, CVs; *circles*, MSPs; *diamonds*, active binaries; *X mark*, qLMXB; *asterisk*, unknown). Subsequent figures use the same labeling.

available ($W15_{opt}$, $W33_{opt}$, $W45_{opt}$, and $W70_{opt}$), we have assumed that the object is found on the MS in the V versus $V-I$ CMD. As expected, significantly higher rms values than average are found for stars with large-amplitude, periodic variations (e.g., $W1_{opt}$, $W8_{opt}$, and $W15_{opt}$). Among the CV candidates, significant nonperiodic variations were found for V1, V2, V3, and $W25_{opt}$. These objects are clearly visible in the V and I images, and are not affected by diffraction spikes or saturation trails, so the source of the enhanced noise for these objects is probably flickering from the hot spot or accretion disk. Strong temporal changes in the PSFs correlated with telescope breathing caused likely spurious signals to appear in the power spectra near the *HST* orbital frequency (0.1725 mHz) for these four large-amplitude variables.

The same explanation cannot be confidently applied to the possible enhanced noise for $W33_{opt}$, $W45_{opt}$, $W70_{opt}$, and $W120_{opt}$. These objects are all so crowded that none of them were detected in the original V and I band images by AGB01, and the enhanced noise could have some contribution from this crowding. Strong signals near the *HST* period are only found for $W33_{opt}$ in the I band. By contrast, the ID for $W44_{opt}$ is relatively isolated, although faint, and the higher rms values found here are also suggestive of nonperiodic variations.

2.2.2. *GO-7503 Data*

Significant variability was found for several of the CV candidates by comparing the third-epoch images of the *HST* program GO-7503 with those obtained in the first two epochs (epoch 1, GO-5912; epoch 2, GO-6467). Figure 9 shows those cases in which F300W variability was discovered (small amplitude variability was also found for V2, a known DN, but is not shown here). Most of the variations are obvious from Figure 9, with the exception of $W44_{opt}$, which is 0.36 mag fainter in the first epoch than it is in the second (and 0.30 mag fainter in the first than in the third), and $W122_{opt}$, which is 0.87 mag fainter in the first epoch than the second and 0.52 mag brighter in the second epoch than the third. Some of these variations may represent DN outbursts, especially $W51_{opt}$ and $W56_{opt}$. A detailed analysis of the long-term variability of the CVs will be deferred to a later publication (where these results will be combined with subsequent *HST* observations made with the Advanced Camera for Surveys [ACS]).

2.2.3. *Period-M_V Plot*

Having a sample of CVs and CV candidates with period and M_V determinations at a well-known distance allows us to examine the period-luminosity relationship expected for CVs. Figure 10*a* shows a plot of period versus M_V for CVs and CV candidates in 47 Tuc along with those of CV1 and CV6 in NGC 6397 (Grindlay et al. 2001b, hereafter GHE01b; Kaluzny & Thompson 2002), the DN in M5 (Neill et al. 2002), two CVs in NGC 6752 (Bailyn et al. 1996), and the magnetic CV in M67 (Gilliland et al. 1991). The straight line is equation (1) from Warner (1995), for solar-metallicity stars. This will shift to brighter magnitudes (by about 1 mag) for metal-poor secondaries, so CVs that are near or above this line are likely to have evolved secondaries. Some of the V-band light will be from the accretion disk and hot spot (as well as the secondary), and this will also push the V magnitudes to brighter values (to the left in

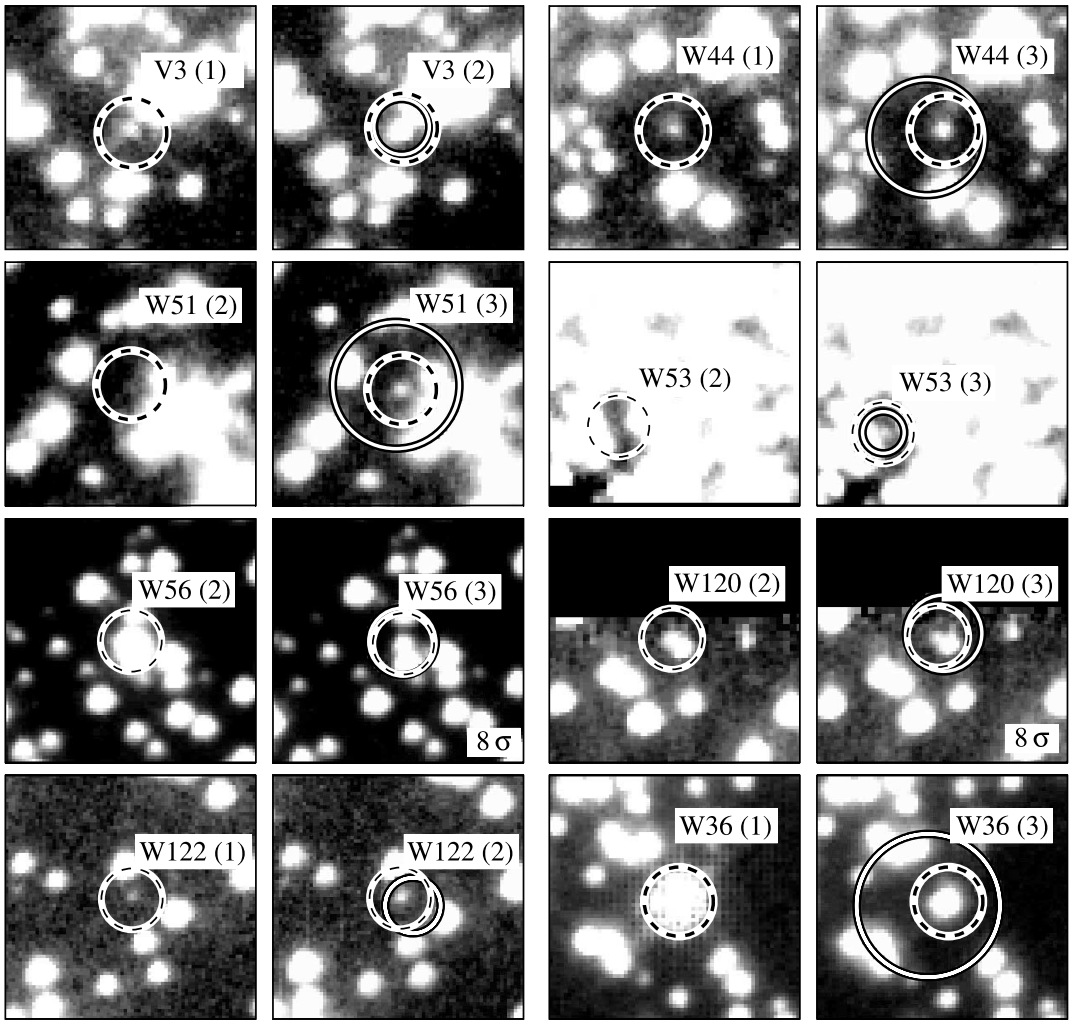

FIG. 9.—Finding charts (in F300W) for the CVs or CV candidates found in the GO-7503 FoV that show detectable or significant long-term variability. Data from GO-5912 (epoch 1), GO-6467 (epoch 2), and GO-7503 (epoch 3) are shown (the appropriate epoch number is shown in parentheses). The solid lines show the 4 σ error circles (except in the cases of W56 and W120, where 8 σ error circles are shown for clarity), and the dashed circles encircle the IDs (with radius 0.″2 for PC1 and 0.″1 for the WF chips).

Fig. 10*a*). Figure 10*b* shows the plot for the blue variables described earlier.

The likely CV $W2_{opt}$ and the CV candidate V3 both lie close to or above the MS ridgeline in the V versus $V-I$ CMD (see the CMD for PC1 in Paper I), showing that the secondary dominates the optical light. As expected, these objects lie close to the Warner relationship. The secondary for $W2_{opt}$ might be evolved, but better photometry is needed to make this conclusion secure. The CVs V1 and $W1_{opt}$ fall below equation (1) because the accretion disk and hot spot (and possibly the WD) make significant contributions to the light (the CMDs in Paper I show that the $V-I$ colors of $W1_{opt}$ and V1 are well to the blue of the MS). The light curve of the eclipsing CV $W15_{opt}$ (Fig. 2) implies that the accretion disk and hot spot are responsible for $\sim$60% of the V-band light, and increasing V by $\sim$1 mag to isolate the MS component brings $W15_{opt}$ into excellent agreement with equation (1). For $W8_{opt}$, around 40% of the V-band light appears to come from a source other than the secondary. Given the similarity of the light contributions from the secondaries, equation (1) implies that the $W8_{opt}$ secondary should be about 2 mag fainter than the $W15_{opt}$ secondary, but instead it is almost 1 mag *brighter*. Possible explanations are that (1) we are seeing a grazing eclipse with the inclination slightly less than 90°, (2) a faint MS star is contaminating the light from the CV, or (3) the normalization for $W8_{opt}$ is incorrect because of the crowding. Examination of Figure 2 shows that the ellipsoidal variations in $W15_{opt}$ are close to the maximum value expected (see Russell 1945), but are around a factor of 2 smaller in $W8_{opt}$, consistent with any of these three explanations. Similar (but less extreme) issues exist for the two NGC 6752 CVs (both of these systems lie close to the MS in the V vs. $V-I$ CMD). The good agreement of the M5 DN with equation (1) implies that the V-band light must be dominated by the secondary.

The variable $W34_{opt}$ has colors that are consistent with those of a CV ($U-V=-0.12$, $V-I=1.03$, $M_V=9.3$) and appropriately falls below equation (1). However, as noted by Edmonds et al. (2002a), the relatively large amplitude variation of this object in both V and I makes an MSP another possibility, since the light curve is similar to that of $W29_{opt}$ (47 Tuc W). Either possibility is consistent with the X-ray properties of this object. The variable $W21_{opt}$ ($U-V=0.15$, $V-I=0.27$, $M_V=7.44$) is also difficult to

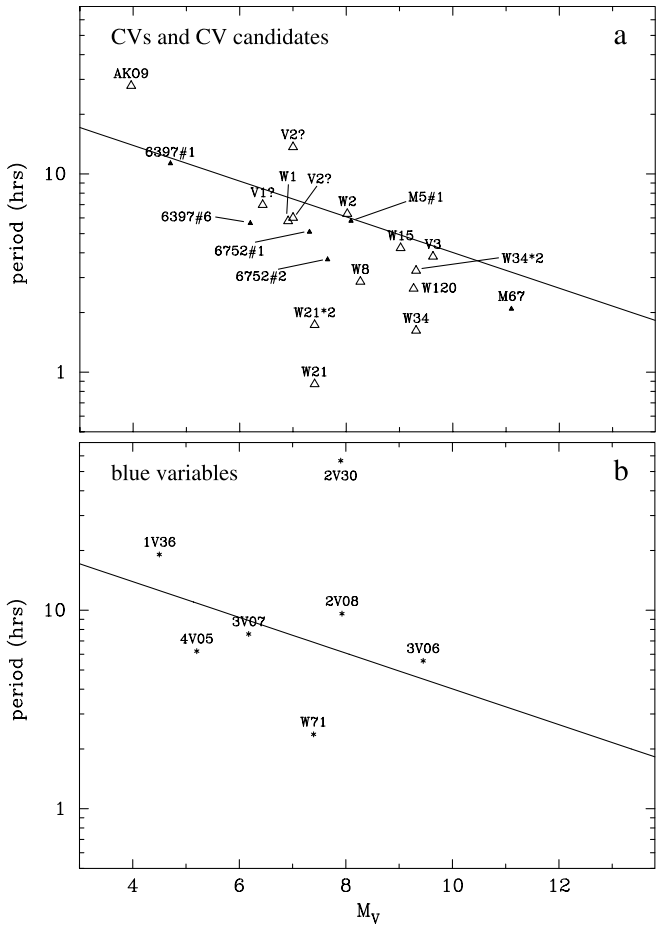

FIG. 10.—Plot of orbital period vs. M_V for (*a*) 47 Tuc CVs and CV candidates and (*b*) blue variables. In (*a*) two CVs from each of the globular clusters NGC 6397 (CV1 and CV6; Grindlay et al. 2001b; Kaluzny & Thompson 2002) and NGC 6752 (Bailyn et al. 1996) are shown, plus a CV from M5 (Neill et al. 2002) and M67 (Gilliland et al. 1991). Small filled triangles are used to plot the non–47 Tuc CVs. The periods for the blue variables have been assumed to be twice those found from the peak in the power spectrum. The straight line shows eq. (1) from Warner (1995).

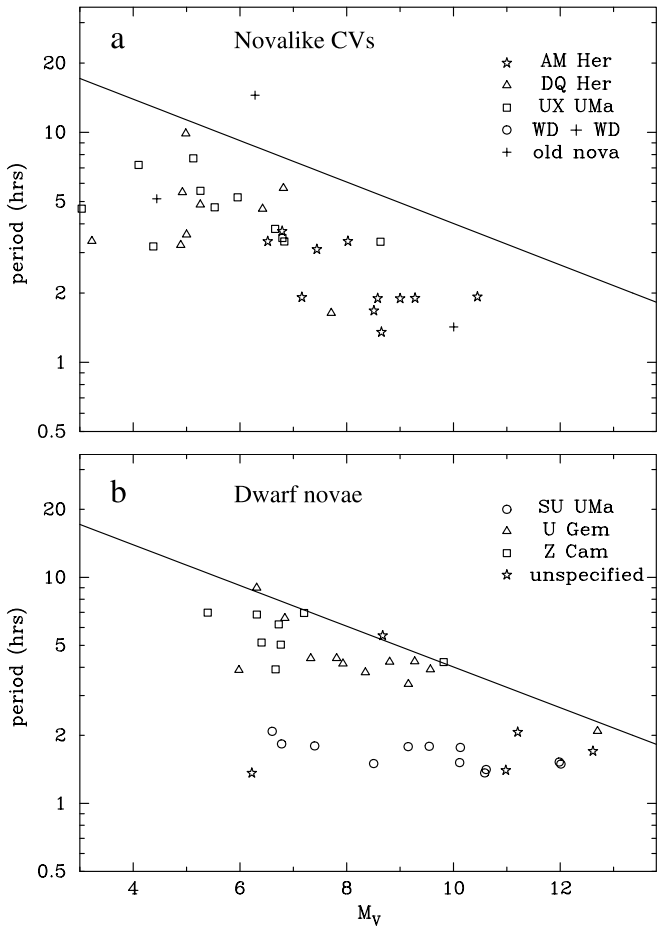

FIG. 11.—Plot of orbital period vs. M_V for field CVs from VBR97, for (*a*) nova-like systems and (*b*) DN systems.

categorize. Assuming that the orbital period is twice the observed period, the star still falls well below equation (1). Could an accretion disk for a CV with a period of 1.73 hr and an expected $M_V(2) = 14$ be this bright? Figure 9.8 of Warner (1995) shows that the 13 dwarf novae (DNe) with periods $\lesssim 2$ hr mostly have $M_V(\mathrm{disk}) = 8$–9, with three having $M_V(\mathrm{disk}) \lesssim 7.1$. However, we would expect a very blue $U-V$ color if the disk is this bright. Alternatively, the binary could be a WD-WD CV or a WD-NS system in quiescence. Finally, AKO 9, with its subgiant secondary, is well outside the range of applicability of equation (1).

Figure 11 shows a period versus M_V plot (similar to Fig. 10) for the field CVs with estimated distances in the *ROSAT* study by VBR97. The orbital periods have been taken from Ritter & Kolb (1998). The nova-like CVs (systems that are magnetic or do not show outbursts) and the DNe (outbursting systems) have been separated into two plots to show systematic differences between these two general classes of CV. The labeling of VBR97 for the different CV types is used. The nova-like CVs are generally farther away from equation (1) than the DNe, showing that the relative light contributions from the accretion disk and hot spot (compared to the secondary) are larger than for the DNe. The 47 Tuc CVs (and the other cluster CVs) appear to be more consistent with the DNe from VBR97 than the nova-like systems.

By calculating the magnitude predicted by equation (1) (using the binary period) and subtracting M_V, we quantify the offsets from equation (1) and examine the light contribution from sources other than the secondary (mainly the accretion disk, hot spot, and WD). This procedure will overestimate the contribution from the disk and other nonsecondary components, since equation (1) underestimates the contribution from a metal-poor secondary. Figure 12 shows the cumulative distributions of the offsets from equation (1) for the 47 Tuc and the field CVs. We have eliminated binaries with periods of greater than10 hr to remain consistent with the period limitations on equation (1). Figure 12*a* shows all such systems, and Figure 12*b* shows only systems with periods above the CV period gap (the latter figure avoids the shortest period systems, likely to have a greater light contamination from the WD). For systems above the period gap, the offset distributions for the 47 Tuc CVs and the nova-like systems are distinguishable at the 99.55% level using the Kolmogorov-Smirnov (K-S) test. A subset of the nova-like systems, the DQ Her's, are distinguishable from the 47 Tuc CVs at the 93.8% level (the nova-like and DQ Her offsets are distinguishable from each other at the 1.2% level). By contrast, the 47 Tuc CV offsets are distinguishable from the DNe offsets and the U Gem systems at only the 1.4% and 0.9% levels, respectively. This suggests

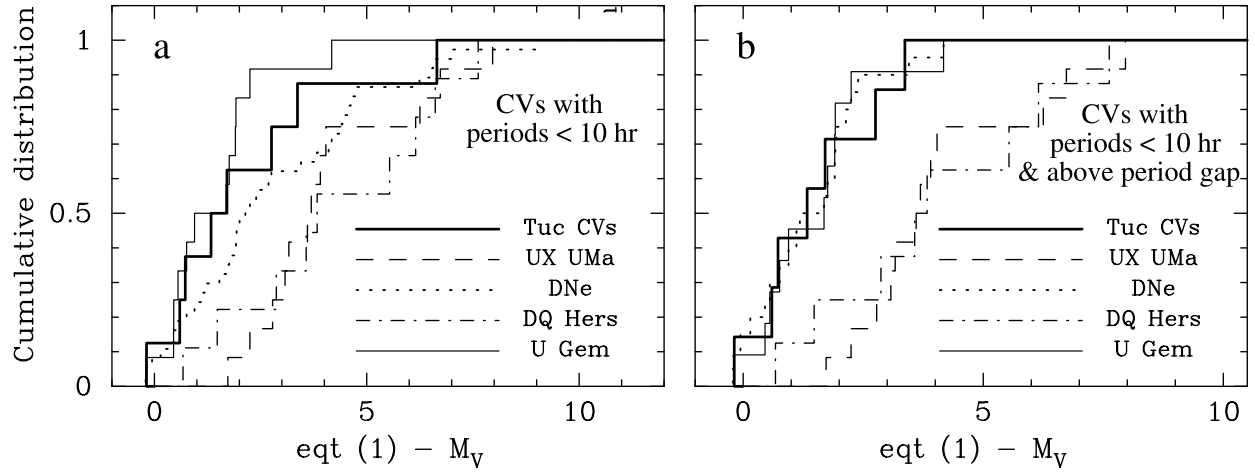

FIG. 12.—Cumulative plots of the difference between M_V predicted by eq. (1) (using the binary period) and the measured M_V for 47 Tuc CVs (labeled as "Tuc CVs") compared to field CVs from VBR97. This difference is an estimate of the brightness of the accretion disk and hot spot, plus (for faint systems) the WD, where higher accretion luminosities are toward the right of the figure. The secondaries in the 47 Tuc systems will be brighter than solar metallicity secondaries, and so the 47 Tuc accretion luminosities will be even fainter than shown by these figures. The "DNe" distribution is for all DN systems. Panel *a* shows all systems with periods less than 10 hr, and panel *b* shows systems with periods less than 10 hr but above the CV period gap (this shows systems in which the contribution from the white dwarf is likely to be smaller).

that the 47 Tuc CVs have accretion luminosities that are even lower than those found in U Gem systems and DNe since, as mentioned above, the nonsecondary component in the 47 Tuc CVs is being underestimated here. This then suggests that the 47 Tuc CVs have lower accretion rates. More evidence supporting this conclusion is given in § 3.2, and discussion is given in § 4.1.

2.3. *Blue Variables*

As described in Paper I, several blue, variable stars discovered by AGB01 are not obviously associated with X-ray sources and have colors that are different from most cluster and field CVs. The time series for these blue variables are shown in Figure 13, and the period versus M_V plot is shown in Figure 10*b*. The variable 1V36 has a sinusoidal, 9.55 hr variation; 2V08 and 2V30 have 4.8 hr and 28.3 hr variations, and 3V06, 3V07 and 4V05 have 2.78 hr, 3.79 hr, and 3.11 hr variations, respectively. Note that the absolute magnitudes of the secondaries (if MS members) are likely to be significantly fainter than the observed M_V because these stars are all blue in V versus $V-I$. We have assumed that the orbital period is twice the detected period, as appropriate for most CVs (Roche lobe filling, MS secondaries with ellipsoidal variations) with periodic variations detected in the optical. If this assumption is correct, then 1V36, 2V08, 2V30, and 3V06 are unlikely to be filling their Roche lobes, since they fall above equation (1) in Figure 10*b*, and are therefore unlikely to be CVs (as already noted for 1V36 by AGB01). If any of the secondaries are evolved then they could fill their Roche lobe at the observed period, but such secondaries should be unusually red, and therefore to explain the observed blue $V-I$ colors we probably require an unusually UV-bright, luminous component. Even if evolved companions were expected to give unusually bright disks, only 2V08 and 2V30 have $U-V$ colors as blue as most of the other CVs, so the blue variables do not seem to have unusually bright disks. The blue color for 3V07 implies that only a small fraction of the optical light comes from a MS star, and therefore the secondary for this system is also likely to fall above the Warner relationship (the M_V offset of 3V07 from eq. [1] in Fig. 10 of $\sim$1 mag roughly equals its offset from the MS in the V vs. $V-I$ CMD).

Another possibility is that the orbital periods are the same as the observed periods, and that the variations are caused by the heating of one side of an MS star. In this case, some of the blue variables (like 1V36) may not have to contain evolved secondaries for Roche lobe filling to be taking place. There are at least two problems with this explanation. First, a UV-bright, relatively luminous component is probably required to cause measurable heating effects, but only 2V08 and 2V30 have $U-V$ colors that are comparable to those of the bluest CVs. Second, because sinusoidal signals with low amplitudes (either from heating or ellipsoidal variations) are generally not detectable even in the brightest CVs because of noise from flickering. If the blue variables are CVs, then we would expect flickering to mask the small sinusoidal signals that are observed. Instead, the rms values for the blue variables are quite low (Fig. 8), implying low-amplitude flickering, despite having bluer colors and (presumably) relatively bright disks, if they are CVs.

We note that these results are unlikely to be some sort of photometric artifact (such as the effects of bad pixels), since several of these objects exist and none of them show unusual PSF fits, or excessive levels of crowding. Also, the power spectra show little if any extra power near the *HST* orbital frequency. See § 3.4 for more discussion of these unusual objects.

2.4. *Active Binaries*

The phase plots for $W12_{opt}$, $W92_{opt}$, $W137_{opt}$, and $W182_{opt}$ (eclipsing binaries); and $W41_{opt}$, $W47_{opt}$, and $W163_{opt}$ (contact binaries) are shown in AGB01. Light curves for most of the BY Dra's and red stragglers from AGB01 that have also been identified as active binary candidates are shown in Figure 14, and phase plots for a selection of active binary candidates not found by AGB01 are shown in Figure 15. Note that ambiguity exists in the period deter-

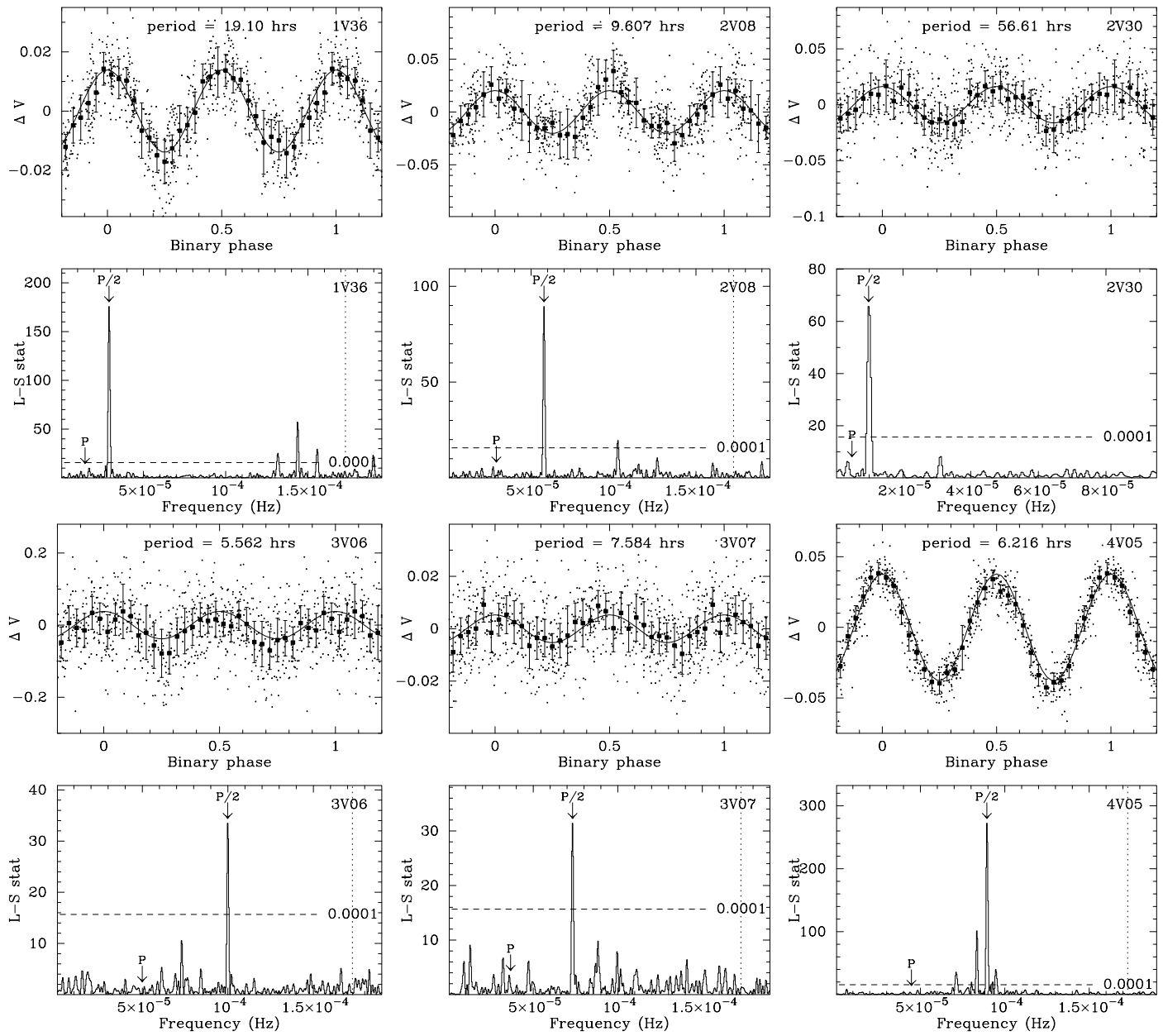

FIG. 13.—Phase plots and power spectra in the *V* band, for the blue variables from AGB01. In each case the orbital period has been assumed to be twice that derived from the peak in the power spectrum. Sinusoidal fits to the data are shown. The marginal optical counterpart to W71, another blue variable, was previously shown in Fig. 4.

mination for several of the variables shown in Figure 15 (especially for $W22_{opt}$ and $W94_{opt}$). In these cases, we have assumed that the orbital period is twice the observed period. Clearly, $W38_{opt}$ and $W94_{opt}$ are eclipsing binaries, and the other new objects are likely a mixture of BY Dra and W UMa systems ($W66_{opt}$ was classified by AGB01 as a noneclipsing contact binary).

3. ANALYSIS

3.1. *Radial Distribution of Sources: Comparison between Source Classes*

Here we compare the radial offsets, with respect to the center of 47 Tuc ("radial distributions") of the different classes of binary. Although the GO-7503 data set has uncovered a number of likely CVs and at least two active binary candidates, for radial distribution analysis we restrict ourselves to the GO-8267 data set because it contains a much more complete sample of active binary candidates. Figure 16 shows the radial distributions of (1) the radio-detected MSPs (plus W34), (2) the CVs, (3) the binaries discovered by AGB01 (with the relatively small fraction of X-ray–bright systems and the two confirmed CVs removed), (4) the candidate active binaries or "xABs" (MS or red straggler binaries from either AGB01 or this work with apparent X-ray counterparts), and (5) the blue variables. Note the similarity between the CV and the MSP radial distributions (K-S test probability 14.0%). This similarity is not surprising, because the single MSPs should have masses of $\sim$1.4 $M_\odot$ and the MSP binaries only $\sim$0.02–0.2 $M_\odot$ more. The detected CV candidates should have masses ranging

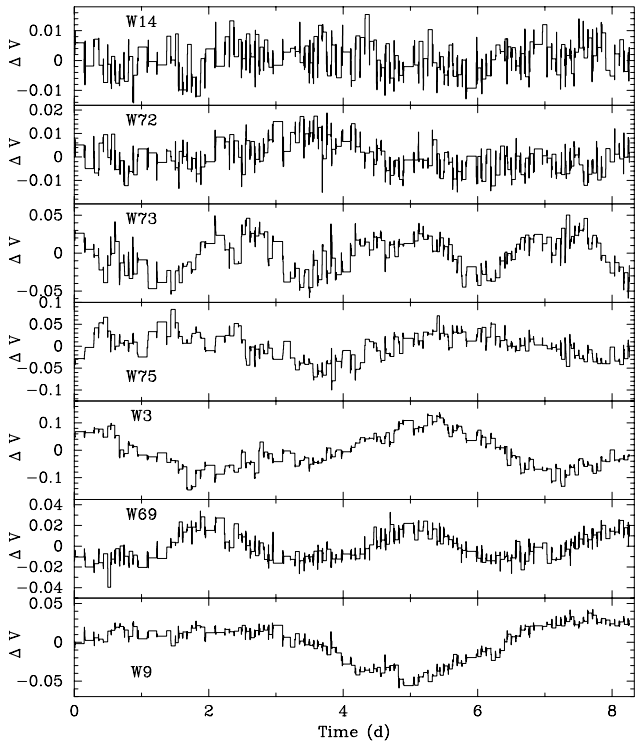

FIG. 14.—Time series for a sample of active binaries with long periods. These are a mixture of red stragglers ($W3_{opt}$ and $W72_{opt}$) and red straggler candidates ($W14_{opt}$), binaries and likely BY Dra variables located near or above the MSTO ($W9_{opt}$, $W73_{opt}$, and $W75_{opt}$), and a variable located well above the MS ridgeline ($W69_{opt}$). Short horizontal segments in the time series show various gaps in the time series.

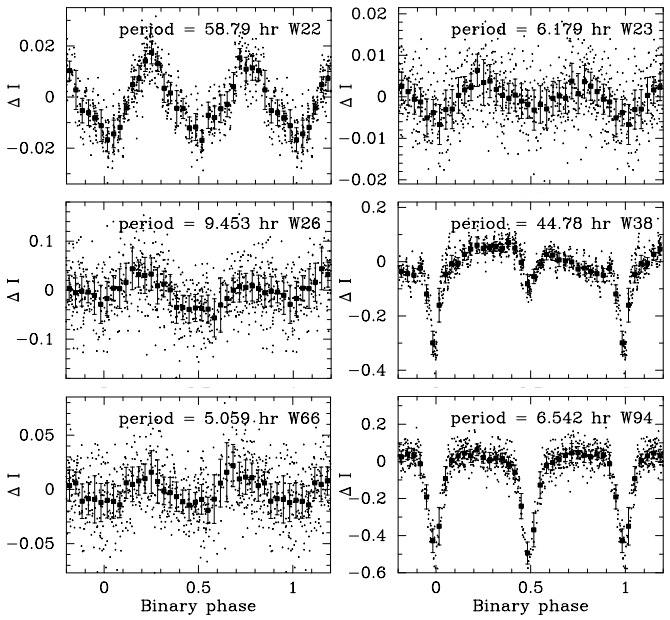

FIG. 15.—Phase plots for a sample of active binaries not found by AGB01 (because of crowding), plus the faint variable $W66_{opt}$

from ~0.95 $M_\odot$ for faint objects like V3 and $W120_{opt}$ (~0.4 $M_\odot$ secondary and ~0.55 $M_\odot$ primary) up to ~1.6 $M_\odot$ for AKO 9 (~0.8 $M_\odot$ primary and secondary). The seven blue variables are slightly less centrally concentrated than the CVs (K-S test probability 88.2%) and the MSPs (K-S test probability 93.8%). Eliminating 2V08 and 2V30, the two

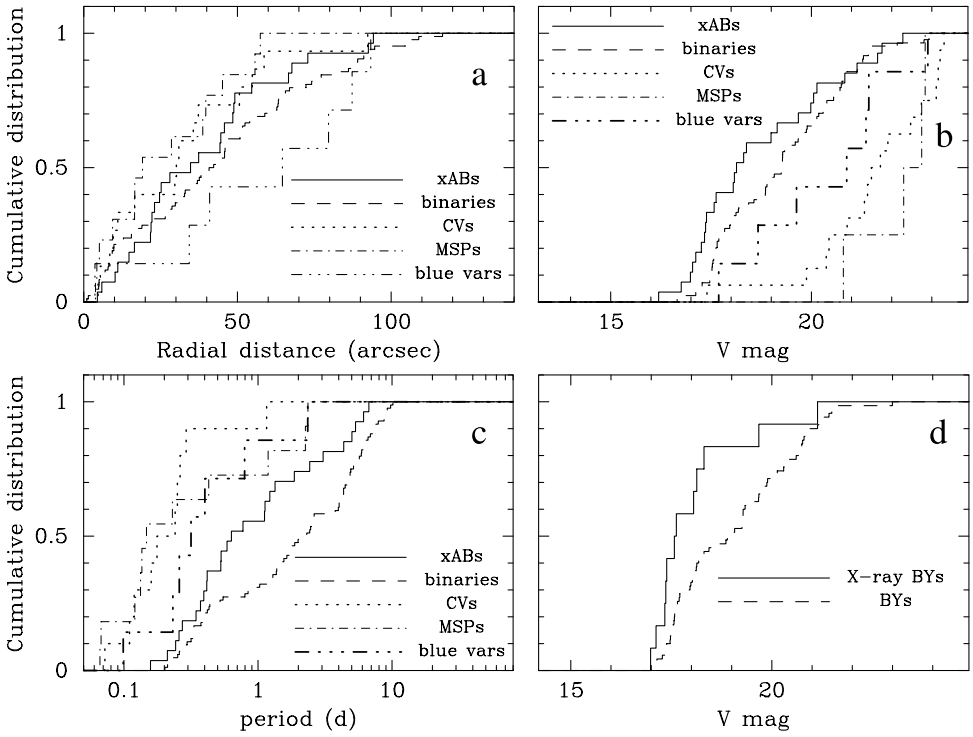

FIG. 16.—Cumulative radial distributions for several classes of 47 Tuc binary. (*a*) CVs, MSPs, binaries detected by AGB01 ("binaries"), the subset of these binaries ("xABs") detected in X-rays, and the blue variables. (*b*) *V* distribution of this same subset of binaries, where the MSP list includes only 47 Tuc U, 47 Tuc W (W29), W34, and the possible ID for 47 Tuc T. (*c*) Period distribution for these binaries, where the periods are derived from AGB01, Camilo et al. (2000), and this work. (*d*) *V* distribution for the AGB01 binaries classified as BY Dra systems and the subset of these systems that are X-ray sources.

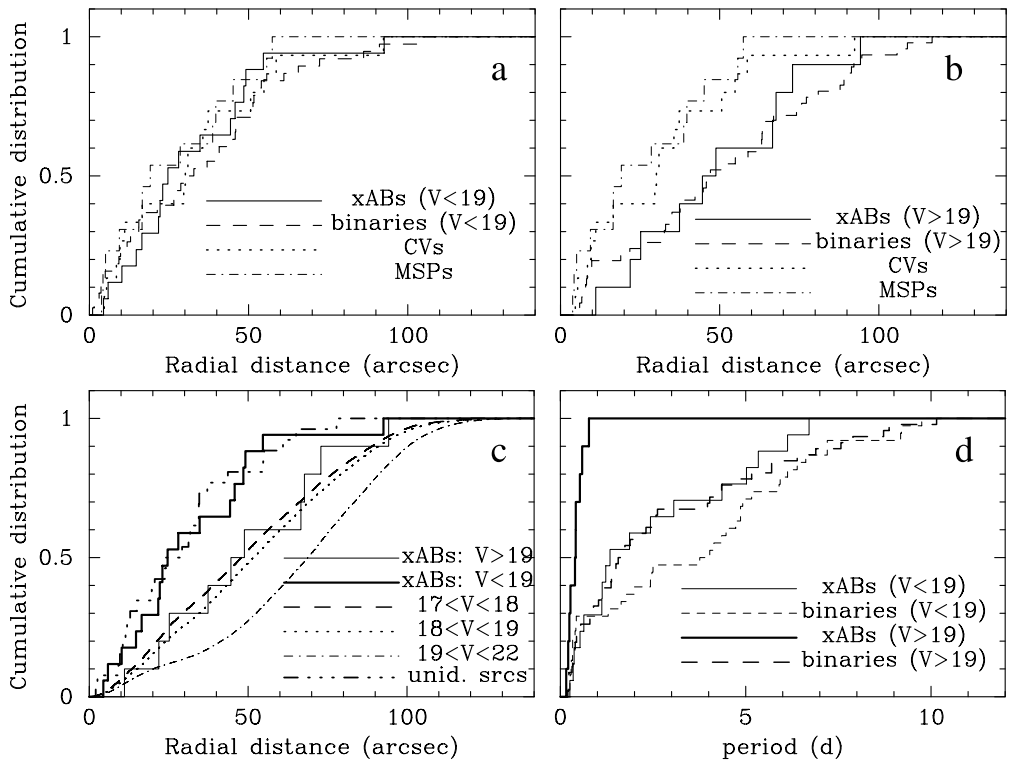

FIG. 17.—Radial distributions for (*a*) bright ($V < 19$) and (*b*) faint ($V > 19$) subsets of the AGB01 binaries and the active binaries. Also shown are (*c*) the radial distributions of the bright and faint active binaries, the total stellar population (mostly single stars) in the quoted V ranges, and the unidentified X-ray sources in the GO-8267 field of view; and (*d*) the period distributions for the bright and faint AGB01 binaries and the active binaries.

variables with colors most like white dwarfs or CVs, causes the above K-S test probabilities to drop to 53% and 55%, suggesting that the blue variables are heavy objects (2V08 and 2V30 are relatively distant). However, the remaining sample of five is very small for statistical tests.

The radial distribution of the AGB01 binaries is slightly less centrally concentrated than those of the CVs and MSPs (K-S test probabilities of 77% and 81%, respectively). These results are only marginally statistically significant, but are a likely result of lower masses for some of the AGB01 binaries, especially the faintest ones. The active binaries appear to be marginally more centrally concentrated than the AGB01 binaries, but the K-S test probability (45%) is not statistically significant. If real, this difference likely results from the generally brighter V magnitudes (and higher masses) of the active binaries compared to the AGB01 binaries (see Fig. 16*b*), since the V distributions differ at the 90% probability level. Also, the V magnitudes of the X-ray–bright BY Dra's are brighter than the V magnitudes of the much larger BY Dra population from AGB01 (see Fig 16*d*; K-S test probability 93.5%). The active binary periods extend to higher values than the periods of the CVs and the MSPs (Fig. 16*c*), and most strikingly they are significantly shorter than those of the AGB01 binaries (K-S probability 98.9%).

We now consider the AGB01 binaries and active binaries with $V < 19$ and $V > 19$ (this divides the AGB01 binaries into two evenly sized groups). In the bright subsample, the radial distributions of the AGB01 binaries and the active binaries are indistinguishable from each other (K-S test probability 16%). The radial distributions of both the AGB01 and the bright active binaries are indistinguishable from those of the MSPs (K-S test probabilities 30% and 29%) and CVs (K-S test probabilities 16% and 9%; see Fig. 17*a*).

Considering the fainter binaries ($V > 19$), the radial distribution of the faint AGB01 binaries and the faint active binaries are indistinguishable from each other (K-S test probability 12%). The radial distributions of both the faint AGB01 binaries and the faint active binaries (see Fig. 17*b*) are less centrally concentrated than those of the MSPs (K-S test probabilities 97.0% and 83%), with similar results for the CVs (K-S test probabilities 93% and 85%). These results are consistent with the faint active binaries being less massive than the bright active binaries.

Figure 17*c* shows the radial distribution of the sources in the GO-8267 FoV that have not been identified, plotted with the bright and faint active binaries and the general stellar population in three different V-band ranges. The unidentified sources are indistinguishable from the bright active binaries, the CVs and the MSPs, showing that they are consistent with any of these groups, or a combination of all three types. The faint active binaries have a radial distribution that is almost identical to that of the stars with $17 < V < 18$ (probability 0.73%), and is considerably more concentrated than the stars with $19 < V < 22$ (probability 84.7%). All of these results are consistent with expectations for mass segregation of binaries and stars in 47 Tuc, and with the statement of AGB01 that incompleteness as a function of radius and magnitude is expected to be small even for stars as faint as $V \sim 21.5$.

The most striking result is that the period distribution of the faint active binaries differs from that of the faint AGB01 binaries at the 99.99% probability level. Figure 17*d* shows

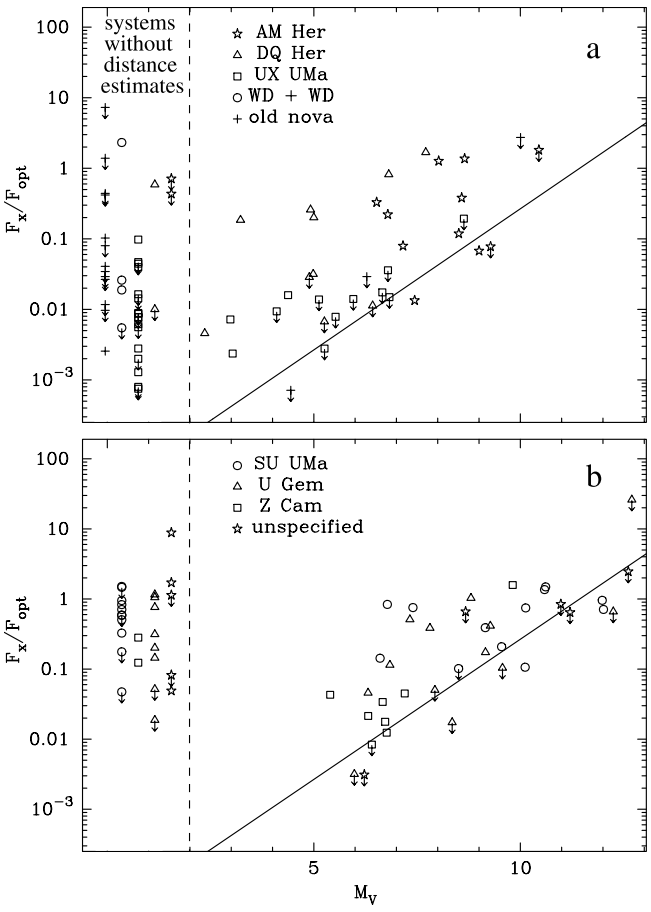

FIG. 18.—Plots of F_X/F_{opt} vs. M_V for the field CVs from VBR97, for (*a*) nova-like CVs and (*b*) the DNe. Field systems are plotted where the distance is known; otherwise the systems are shown in the left portion of the figures. The straight line shows $L_X = 10^{30}$ ergs s^{-1}.

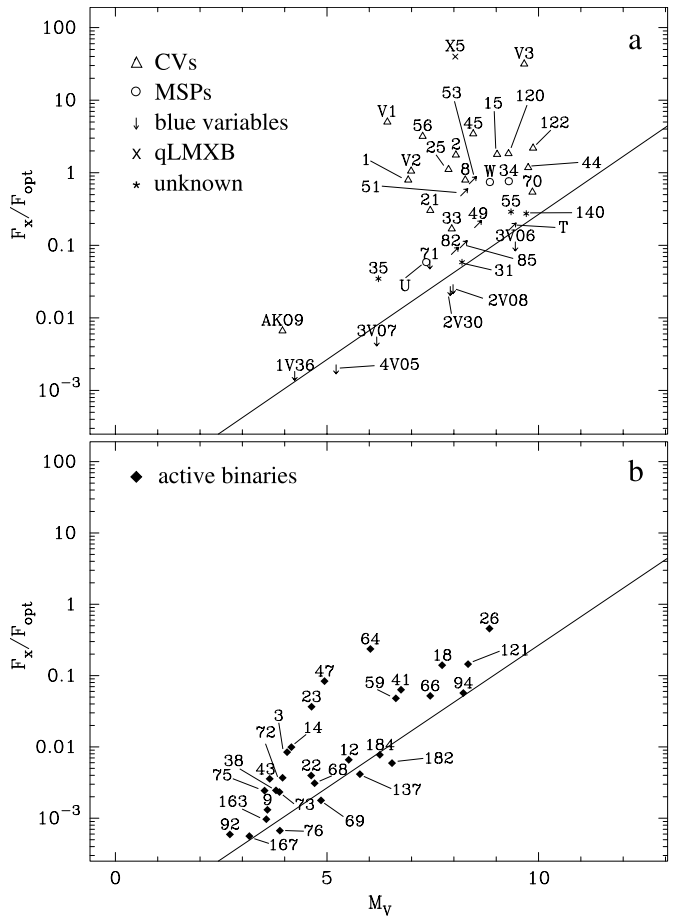

FIG. 19.—Plots of F_X/F_{opt} vs. M_V for the 47 Tuc optical identifications of *Chandra* sources. The symbols used as the same as Fig. 8, except that arrows are shown for limits in F_X (blue variables) or M_V (faint CVs in GO-7503 and 47 Tuc T).

that while *all* of the faint active binaries have periods $\lesssim 0.7$ days, only $\sim$30% of the AGB01 binaries have periods below this value. We discuss in § 4.2 how these results imply the presence of a stronger relationship between luminosity and period than found in field objects.

3.2. *X-Ray–to–Optical Flux Ratio*

3.2.1. *Comparison between Source Classes*

A useful, distance-independent diagnostic for stars detected in both the optical and X-ray wavelength bands is the ratio of the X-ray flux to the optical flux. Figures 18*a* and 18*b* show plots of this ratio versus M_V for nova-like CVs and DNe in the field (VBR97). The F_X values in the 0.5–2.5 keV band from VBR97 were scaled to be consistent with the slightly absorbed, 1 keV thermal bremsstrahlung spectra (0.5–2.5 keV) assumed by GHE01a, and used here. The F_{opt} values were derived from $F_{opt} = 10^{-0.4V-5.43}$. In cases where the distances to the field CVs of VBR97 were unknown, the systems were plotted on the left side of Figures 18*a* and 18*b*.

The majority of field DNe have $F_X/F_{opt} > 0.01$, with the smallest ratios being dominated by Z Cam systems (with relatively high accretion rates). The remaining DN classes (U Gem and SU UMa systems) mostly have $F_X/F_{opt} > 0.1$. Among the nova-like CVs, the UX UMa systems have F_X/F_{opt} values or limits mostly around 0.01. These ranges show a clear trend that higher F_X/F_{opt} values correspond to lower accretion rates for nonmagnetic CVs, as pointed out by VBR97 for this sample of field CVs, and by Richman (1996). Most magnetic CVs have $F_X/F_{opt} > 0.1$, although it is unclear if F_X/F_{opt} is anticorrelated with accretion rate for these systems.

Figure 19*a* shows the F_X/F_{opt} values for the 47 Tuc CV candidates and MSPs (plus other blue IDs) and Figure 19*b* shows the F_X/F_{opt} values for the active binary candidates. Limits are shown where appropriate. Note the clear differences between Figures 19*a* and 19*b*, with generally much larger F_X/F_{opt} values for the CVs and the MSPs. With the exception of AKO 9, the F_X/F_{opt} values for 47 Tuc CVs and CV candidates are all greater than 0.1, suggesting that the population of 47 Tuc CVs, if dominated by nonmagnetic systems, are low accretion rate CVs (U Gem and SU UMa systems, where the latter subclass are believed to have the lowest accretion rates among field CVs). Besides V3, the likely DQ Her system V1 (GHE01a) has the highest F_X/F_{opt} value.

Cumulative distributions of F_X/F_{opt} for the 47 Tuc CVs, active binaries, and MSPs are compared in Figure 20*a*. Only the objects detected in V have been included, rather than those with limits, with the exception of 47 Tuc T. The clear differences between the CV and the active binary

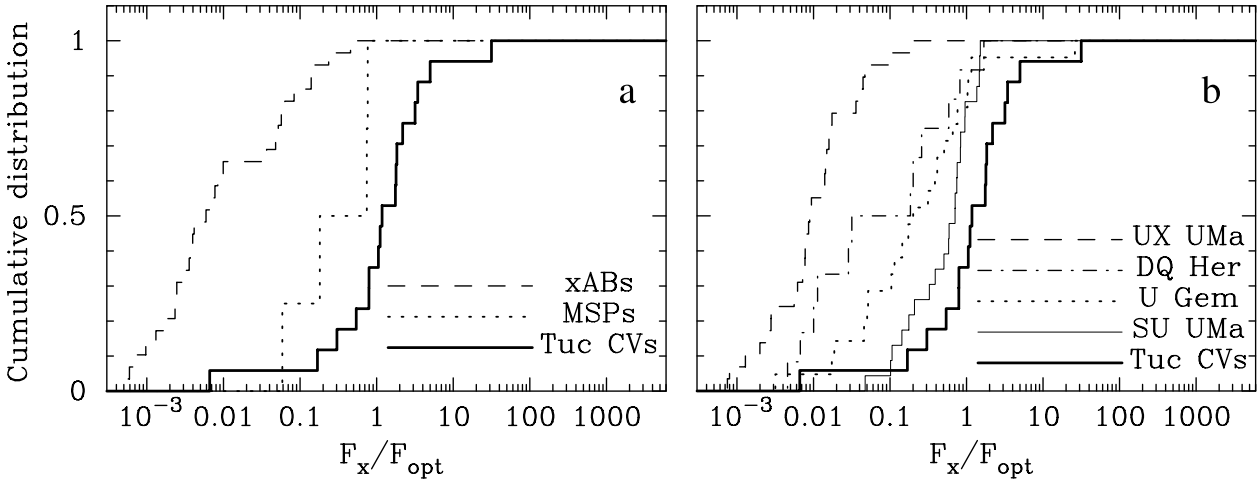

FIG. 20.—Cumulative plots of F_X/F_{opt} for the 47 Tuc CVs compared to (*a*) the 47 Tuc active binaries and MSPs and (*b*) various classes of field CV from the work of VBR97. For the nonmagnetic field CVs, the accretion rates decrease from left to right. These results imply that the nonmagnetic CVs in 47 Tuc have low accretion rates, although the F_X/F_{opt} values are biased by the unusually high L_X values for the 47 Tuc CVs.

TABLE 1

F_X/F_{opt} VALUES FOR 47 TUC SOURCES AND FIELD CVS

Source Type	Number	F_X/F_{opt} (median)
xAB	29	0.0059
MSP	4	0.46
CV	17	1.18
Field CVs[a]		
UX UMa	9	0.0072
Z Cam	9	0.043
AM Her	9	0.22
DQ Her	8	0.23
U Gem	13	0.39
SU UMa	18	0.73

[a] CVs from the study of Verbunt et al. 1997.

distributions (and between the MSP and active binary distributions) are confirmed by the median values given in Table 1 and the large K-S test probabilities shown in Table 2. The MSP distribution only contains four systems, and the other binary MSPs detected in the radio fall below our optical detection threshold (but are mostly detected by *Chandra*), so the true MSP distribution will extend to higher F_X/F_{opt} values. The only region of significant overlap between the active binaries and either the CVs or MSPs is found with $0.1 < F_X/F_{opt} < 0.5$. All of these apparently extreme active binaries are found in the faint group and have radial distributions that are less centrally concentrated than either the CVs, the MSPs, or the bright active binaries.

3.2.2. *Cataclysmic Variables*

In Figure 20*b* the 47 Tuc F_X/F_{opt} distribution for the CVs is compared with those found for field CVs using the data given in VBR97. Table 1 shows the median values for each distribution, and Table 2 compares the K-S test probabilities. The trend of increasing F_X/F_{opt} for decreasing accretion rate (Richman 1996; VBR97) is clear, with the UX UMa (nova-like) systems and the SU UMa (DNe) systems at opposite ends of the range, and the Z Cam and U Gem systems falling in between. The 47 Tuc F_X/F_{opt} values are higher on average than all of the various CV subgroups, including three old novae and three double-degenerate systems not shown in Tables 1 and 2. In a separate calculation we have also included the field systems with X-ray limits (rather than just detections) given by VBR97, and this only increases the differences between the F_X/F_{opt} values of the 47 Tuc CVs and the field CVs.

To further investigate the origin of differences in F_X/F_{opt} between the 47 Tuc CVs and the field CVs, we plot in

TABLE 2

K-S TEST PROBABILITIES FOR F_X/F_{opt} DISTRIBUTIONS BEING DIFFERENT

Source	SU UMa	U Gem	DQ Her	AM Her	Z Cam	UX UMa	CV	MSP
U Gem[a]	77.39							
DQ Her[a]	86.13	13.40						
AM Her[a]	97.06	42.68	0.82					
Z Cam[a]	99.84	99.13	87.52	92.22				
UX UMa[a]	100.00	99.99	99.26	99.65	98.13			
CV[b]	97.72	98.20	93.36	98.44	99.93	100.00		
MSP[b]	41.28	1.13	1.43	4.57	90.46	99.11	97.97	
xAB[b]	100.00	100.00	99.73	99.93	99.74	8.17	100.00	99.01

[a] CVs from Verbunt et al. 1997.
[b] Optically identified sources in 47 Tuc.

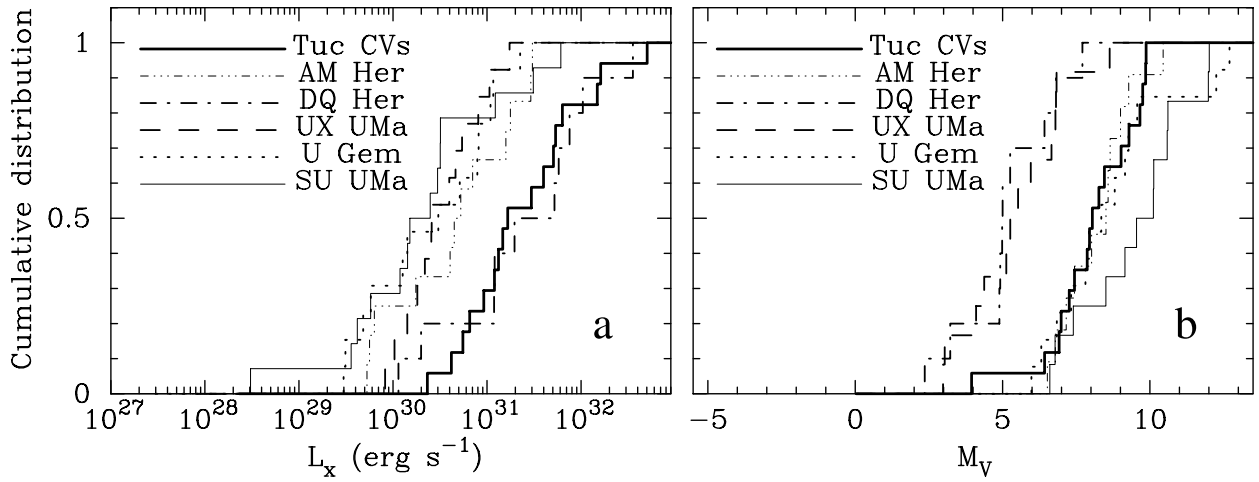

FIG. 21.—Cumulative plots of (*a*) L_X and (*b*) M_V for the 47 Tuc CVs compared to the field CVs from VBR97. Upper limits have been included in the field L_X distributions to increase the sample size. Note the similarity between the L_X distribution of the 47 Tuc CVs and the field DQ Her systems, and the similarity between the M_V distribution of the 47 Tuc CVs and the field U Gem and AM Her systems.

Figure 21*a* the cumulative L_X distributions of the 47 Tuc CVs and field CVs, with a similar plot in Figure 21*b* for M_V. Limits in L_X (corresponding to X-ray detection limits, not distance limits) have been included to increase the sample sizes of the field CVs, since only a subset of the CVs have estimated distances. The luminosities for most of the field CV classes are indistinguishable from each other, with only the DQ Her systems having a significantly different (more luminous) distribution, as pointed out by VBR97. The L_X distribution of the 47 Tuc CVs is distinguishable from the AM Her, DQ Her, UX UMa, Z Cam, U Gem, and SU UMa systems at the 97.6%, 22.4%, 97.3%, 72.2%, 99.3%, and 99.8% levels, respectively, so that only the DQ Her systems are obviously a good match to the 47 Tuc CVs. This would argue against the identification of the 47 Tuc CVs with low accretion rate CVs like DNe, if the accretion rate is proportional to L_X (for example, Warner [1995] suggests $L_{acc} \simeq 50L_X$). However, see the discussion of the M_V distribution below.

Note that the majority of field AM Her and DQ Her systems from VBR97 were X-ray selected (as were the 47 Tuc CVs), unlike other classes of CV, implying that the relatively high X-ray luminosities could be partially selection effects, perhaps weakening the classification of the 47 Tuc CVs with magnetic systems. For example, crowding in X-rays is likely to have prevented the detection of some systems with low X-ray luminosities, and the true cluster distribution will therefore extend to lower luminosities. Robust limits on incompleteness will be presented in future publications. Incompleteness will also apply with the field samples, especially the magnetic systems. For example, although only 2 out of 10 of the DQ Her systems in the field sample analyzed here involve upper limits, a significant number of faint DQ Her's (and other CV classes) may have been missed in field surveys. The four most luminous DQ Her systems are at relatively large distances (>400 pc), suggesting that such bright systems are relatively rare, as pointed out by VBR97. However, despite this incompleteness at low luminosities, the similarity between the 47 Tuc and DQ Her distributions at high luminosities (above ~ 7–8×10^{31} ergs s^{-1}) is noteworthy, and V1, the brightest CV in 47 Tuc, has already been shown to be a likely DQ Her system.

The M_V distribution of the 47 Tuc CVs is distinguishable from the AM Her, DQ Her, UX UMa, Z Cam, U Gem, and SU UMa systems at the 8.6%, 99.97%, 99.99%, 98.80%, 1.03%, and 96.2% levels, respectively. Here, only the AM Her and the U Gem systems are good matches for the 47 Tuc CVs. A comparison of Figures 18 and 19 shows that our optical detection limit of $V \sim 23$ (because of crowding; see § 4.5) is a significant source of incompleteness for faint DNe searches, and may prevent the detection of a significant fraction of SU UMa systems. Clearly, the 47 Tuc CVs are significantly fainter in the optical than the nova-like CVs detected in the field, including the DQ Her systems. Since metal-poor secondaries are expected to be brighter than solar metallicity secondaries, at fixed mass, the difference in accretion luminosity between the 47 Tuc CVs and field DQ Her's will be even more dramatic than suggested by Figure 21*b*. Finally, distances are available for only two old novae, and none are available for double-degenerate systems (both of these classes of CV may be extremely faint and beyond our detection limits).

The faint M_V values for the 47 Tuc CVs suggest that they have low accretion rates, consistent with the period/M_V analysis, but conflicting with the interpretation based on their X-ray luminosities. In fact, an examination of Figure 21 shows that the 47 Tuc CVs have combined L_X and M_V distributions that are not consistent with any known class of field CV (see § 4.1 for discussion of this issue).

3.3. *qLMXB Search*

As expected, the optical ID for X5/W58 (Edmonds et al. 2002b), a qLMXB, has a relatively high F_X/F_{opt} value of 47.8 (Fig. 19; see also Heinke et al. 2003). Interestingly, the CV candidate V3 has a very similar F_X/F_{opt} value. This ratio is higher than that of all known field and 47 Tuc CVs, representing evidence for V3 also being a qLMXB. The possibility that V3 is a binary containing a neutron star has already been discussed by GHE01a, who argue that V3 may

be an enshrouded MSP. For comparison, source B, the possible qLMXB in NGC 6652, has $F_X/F_{opt} \sim 9.0$ when the F_{opt} value given by Heinke, Edmonds, & Grindlay (2001) is appropriately converted, while limits for X7 and the qLMXB in NGC 6397 are >166 (Heinke et al. 2003) and >64, respectively. However, we caution that the *Chandra* and GO-8267 data were not obtained simultaneously, and since V3 is highly variable both optically (see Paper I) and in X-rays (Verbunt & Hasinger 1998; GHE01a), the high F_X/F_{opt} value derived here could be explained by a low optical state during the GO-8267 observations, or a high state during the *Chandra* observations.

The two bright ($L_X \sim 10^{33}$ ergs s^{-1}) sources and likely qLMXBs in 47 Tuc (X5 and X7) and the likely qLMXBs in NGC 6397 and NGC 6440 are all soft sources, using the X-ray color definition of Grindlay et al. (2002), namely, Xcolor = 2.5 log[(0.5–1.5 keV)/(1.5–6 keV)]. Therefore, we have searched for evidence that any of the fainter, soft X-ray sources in 47 Tuc may be qLMXBs (besides V3). The source AKO 9 is a very soft source, but is more likely a CV than a qLMXB because it has been observed to have at least two outbursts without the detection by *ROSAT* or *RXTE* of a 10^{36} ergs s^{-1} source in 47 Tuc (associated with an LMXB in outburst). The only other reasonable candidate is W17, a 103 count source that is a factor of 3 fainter than the qLMXB in NGC 6397. This source is outside the GO-7503 FoV and unfortunately lies in the middle of a large saturation trail in the GO-8267 *V* and *I* images. However, useful limits can be set from the deep and relatively clean *U* image. The nearest detectable stars to the X-ray position are at 2.58, 2.91, and 3.04 σ, and these have $U = 22.4$, 18.3, and 21.1. The fainter two of these are comparable to the CVs $W44_{opt}$ and $W45_{opt}$, and the brighter one to a system intermediate between AKO 9 and V1. We set an upper limit to the detection of a star at the nominal W17 X-ray position (i.e., assuming zero error in transforming to *HST* coordinates) of $U \sim 24$. This is suggestive of a faint optical counterpart like X5 (Edmonds et al. 2002b) or a faint upper limit, as with the qLMXB in NGC 6397 (GHE01b). Other possibilities, besides a qLMXB, are that the source is a soft CV (e.g., an AM Her system) or an active binary. However, for the latter possibility this source would be a factor of ~3 brighter than any of the soft (and nonflaring) active binaries. Follow-up observations with ACS should be useful in searching for optical counterparts and determining the nature of this source.

3.4. *Blue Variables*

As noted in Paper I, 1V36 may be a faint X-ray source ($L_X < 10^{30}$ ergs s^{-1}), arguing in favor of this object being a CV (although Edmonds et al. 2001, 2002a give examples of faint X-ray sources with blue, variable optical counterparts that are MSPs, not CVs). Much deeper *Chandra* observations are required (and have been taken) to confirm this marginal detection of an X-ray source, but there are a number of arguments against the CV identification: (1) the period of 19.1 hr (assuming the observed variations are ellipsoidal) is too long (see Fig. 10)—ellipsoidal variations should be seen in this low noise time series if the system is a CV and therefore Roche lobe filling (unless the inclination is very low); (2) the position of this star in the color-color plot is different from most known field and cluster CVs; (3) the upper limit on F_X/F_{opt} for 1V36 is lower than that of all 47 Tuc CVs (see Fig. 19); and (4) there is no suggestion of the large flickering present in other optically bright CVs such as V1, V2, and $W25_{opt}$. Note that (2) and (4) likely rule out the possibility that several UX UMa systems with very small F_X/F_{opt} values might have slipped beneath our X-ray detection limit. We therefore believe that the comprehensive data available for 1V36 do not support the claim by Knigge et al. (2002a) that 1V36 is a strong CV candidate, and look forward to seeing what STIS/FUV spectroscopy and variability says about this system.

Other explanations for 1V36 fare little better. The variable appears to be too faint and blue in $V-I$ to be a cluster blue straggler, and the star is much too bright to be a horizontal branch or blue straggler star in the SMC. An explanation for this object remains elusive.

All of the other blue variables are uncrowded in the *Chandra* image and consistent with nondetection, and their *HST* time series show no evidence for flickering. As with 1V36, this argues against them being CVs. Here we examine possible alternative explanations for these blue variables: (1) background variable stars from the SMC (e.g., RR Lyrae stars); (2) detached WD binaries; (3) very low accretion rate CVs, like those discussed in Townsley & Bildsten (2002); and (4) exotic collision products. A combination of these may also apply.

Considering possibility (1), we plot two SMC RR Lyrae stars (labeled R1 and R2) in the WF3 CMDs of Paper I. These have periods of 15.2 and 8.7 hr and were independently discovered by two of the authors (Edmonds and Gilliland) using a ground-based variability study of a 47 Tuc field off the core (14.′5 × 14.′5; for background, see Sills et al. 2000). The RR Lyrae light curves have a distinctive asymmetrical appearance that is clearly different from that of the blue variables. Also, only 3V07 lies reasonably close to the expected position of the horizontal branch instability strip. A second possibility is that the variables are pulsating blue stragglers in the SMC. These generally have shorter periods and smaller amplitudes than RR Lyraes, for example the range of periods for the main pulsation modes of the six known SX Phe stars in 47 Tuc are 0.7–2.4 hr and the range of amplitudes is 0.006–0.085 mag (Gilliland et al. 1998). So, while the amplitudes overlap, most of the blue variables have periods that are too long. Also, only 3V07 appears to lie reasonably close to the expected blue straggler sequence. Consistent with these negative conclusions, we note that the number of blue SMC stars above the MSTO in our field is likely to be very small, judging by the detection of only four such stars in the study of a Wide Field Planetary Camera 2 (WFPC2) 47 Tuc field by Zoccali et al. (2001). Proper-motion studies with separate F300W epochs may help confirm the blue variables as 47 Tuc members.

Possibility (2) is attractive because Figure 10*b* shows that several of the blue variables have periods that are reasonably close to, but longer than, the values given by equation (1) for Roche lobe filling. However, only 2V30 has colors that are obviously consistent with those of a MS star/carbon-oxygen (CO) WD binary, and the long period for this system of 1.18 or 2.36 days is difficult to understand as either ellipsoidal variations or heating effects. The colors of 2V08 are very similar to those of a bright WD, so any MS companion is likely to be extremely faint. The other objects with all three colors available (1V36, 3V07, 4V05, and the

possible ID for W71) have colors, compared to the MS, that are bluer in $V-I$ than in $U-V$, behavior that is difficult to reconcile with CO WD-MS star binaries. However, note from the color-color CMD given in Paper I that 3V07 lies very close to the He WD companion to the MSP 47 Tuc U, suggesting that 3V07 may also be a He WD. This does not obviously have an MSP companion, because of the lack of detected X-ray emission, but it could have a WD companion.

Case (3) appears to be an unlikely explanation because the stars are too bright to be consistent with the Townsley & Bildsten (2002) models, and their colors are not obviously consistent with CO WDs. Without having a satisfactory explanation for most of these stars, we turn to possibility (4) that at least some of them represent an exotic collision product formed near the center of 47 Tuc. Mathieu et al. (2002) point out, in their discussion of red stragglers in M67, that stellar encounters are common in star clusters and that it would not be surprising to discover products of such encounters (especially binaries) that run counter to standard evolutionary theory of single stars. Such expectations apply even more so to 47 Tuc.

4. DISCUSSION

4.1. *Cataclysmic Variables*

We have discovered (or confirmed) optical counterparts for 22 *Chandra* sources that are CV candidates, as summarized in Tables 3 and 4 of Paper I. We have included V3 in this list, but, as noted above, it may be a qLMXB. Of these 22 CV candidates, definite variability of some type has been seen for all of them except $W33_{opt}$, $W45_{opt}$, $W49_{opt}$, $W70_{opt}$, $W82_{opt}$, and $W85_{opt}$. The excellent astrometric match between W45 and $W45_{opt}$, the tiny chance of this being a chance coincidence (0.012%), and the relatively bright, hard nature of the X-ray source makes this ID secure. The other candidates have larger possibilities of being chance coincidences (0.8%, 1.0%, 1.4%, 2.3%, and 0.2%) and so without having independent information such as variability or an Hα excess there remains the possibility that one or even more of these five IDs is not real. Also, W70, W82, and W85 are relatively soft sources (Fig. 22), and therefore one or two of them may be MSPs (see § 4.3). Among the marginal candidates, we believe that $W140_{opt}$ and $W55_{opt}$ have the greatest chances of being CVs, as explained in Paper I.

The photometric properties of these stars were summarized in Paper I. The other properties of these systems are summarized as follows: (1) the F_X/F_{opt} values are higher, on average, than those of all classes of CV in the field sample of VBR97, partly because of higher than average X-ray luminosities and partly because of faint optical magnitudes; (2) the periods, where available, are generally consistent with expectations for Roche lobe filling objects; (3) the radial distributions are consistent with those of the cluster MSPs and the brightest MS-MS binaries, and therefore with WD-MS star binaries; and (4) three of the CVs are eclipsing (W8, W15, and AKO 9), several show significant flickering (V1, V2, V3, and $W25_{opt}$), two of them have previously been seen in outburst (V2 and AKO 9), and several others show large amplitude variations (e.g., $W51_{opt}$, V3, and $W56_{opt}$) that may also be signs of outbursts.

The period/M_V data presented in § 2.2.3 and the faint optical magnitudes presented in § 3.2, plus the apparent lack of nonmagnetic nova-like systems, suggest that the 47 Tuc CVs are dominated by low accretion rate CVs, i.e., DNe.[4] This result is not necessarily inconsistent with the lack of outbursts seen for 47 Tuc CVs, since some DNe (such as SU UMa systems) can have quite long recurrence times (Warner 1995). Shara et al. (1996) mention this possibility for 47 Tuc. However, the outbursts seen for V2 and AKO 9, and the possible outbursts shown in Paper I (the GO-7503 variability), do not appear to be as dramatic as those seen in SU UMa systems, and the L_X distributions of the 47 Tuc CVs and field SU UMa's appear to be incompatible. Also, all of the 47 Tuc CVs except for $W21_{opt}$ are found above the period gap, while nearly all known SU UMa systems are found below the period gap. Therefore, we believe it is unlikely that a significant fraction of the 47 Tuc CVs are SU UMa systems.

Selection effects in the field will almost certainly conspire against the detection of low accretion rate CVs (Warner 1995). For example, nova-like systems are relatively bright and blue in the optical. Conversely, SU UMa systems like WZ Sge are extremely faint at optical and X-ray wavelengths, and have very long recurrence times for outbursts. Also, CVs found in the field have a range of nonuniform

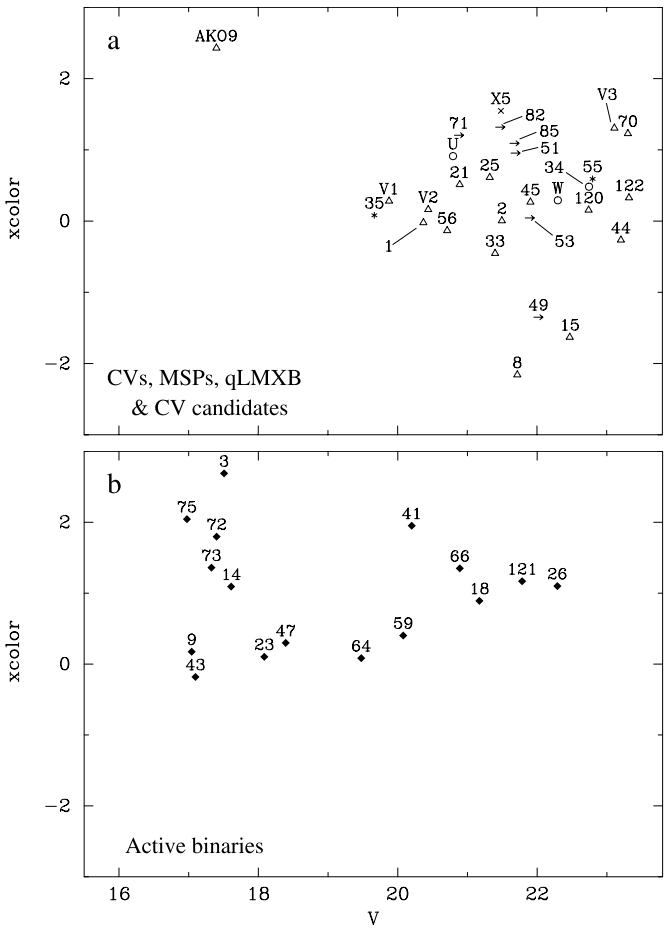

FIG. 22.—X-ray color plotted against V. For the X-ray color we use the definition of GHE01a and the selection criteria of Grindlay et al. (2002) for faint sources. Panel *a* shows the CVs, MSPs, the qLMXB X5 and CV candidates, and panel *b* shows the active binaries.

[4] From § 3.3, it is unlikely that qLMXBs, with their large F_X/F_{opt} values, are significantly biasing our results, since based on X-ray spectral information and F_X/F_{opt} data, only V3 is a reasonable qLMXB candidate.

selection criteria. Although CVs with very low accretion rates (like those modeled in Townsley & Bildsten 2002) will be difficult to detect in 47 Tuc, the sample of cluster CVs is likely to be relatively complete down to X-ray luminosities of 3–5 $\times$ 10^{30} ergs s^{-1}. Therefore, given (1) the depth of our observations, (2) the uniform search methods used, and (3) that the 47 Tuc CVs are effectively all at the same distance, it may be possible that our 47 Tuc CVs are a more representative sample of CVs than the field objects of VBR97, and that they therefore show an expected bias toward lower accretion rate systems.

Is the lower metallicity of 47 Tuc compared to those found in field (Population I) CVs likely to result in lower accretion rates? Stehle et al. (1997) have studied the long-term evolution of CVs with low metallicity secondaries ($Z = 10^{-4}$) and have shown that such systems have a smaller period gap and a slightly higher mass transfer rate than CVs in which the secondary has a solar composition. This trend therefore does not explain the low apparent accretion rates for the 47 Tuc CVs. Population synthesis modeling by Stehle et al. (1997) shows that most Population II CVs should be old enough to have already evolved beyond the period minimum, and will be extremely faint. However, this age effect does not explain the low accretion rates for the 47 Tuc CVs, since the periods for the cluster CVs, where known, are nearly all above the period gap (and most of the CVs with unknown periods should also be found above the period gap).

A potential problem with the low accretion rate interpretation is that no known class of field CV has both L_X and M_V distributions that are similar to those of the 47 Tuc CVs. As noted above, the X-ray luminosities of the 47 Tuc CVs are much higher than those of the U Gem systems, and are consistent with those of DQ Her systems. So, while the faint optical magnitudes imply that they have relatively low accretion rates, the high X-ray luminosities might imply that they have relatively high accretion rates. Only one of these possibilities, at most, can be correct. Since M_V is clearly a better indicator of accretion rate than L_X for nonmagnetic CVs (VBR97), and M_V is also known to strongly depend on accretion rate for magnetic systems (e.g., Hessman, Gänsicke, & Mattei 2000; Yi 1994), we speculate that L_X for the 47 Tuc CVs is a poor guide to their accretion rates whether they are magnetic or nonmagnetic systems. We note that two systems with presumably relatively low accretion rates are V2 (a DN) and $W56_{opt}$, a possible DN. These are two of the brightest CVs in X-rays, with $L_X = 6.3 \times 10^{31}$ ergs s^{-1} and 1.5×10^{32} ergs s^{-1}, respectively, hinting that high X-ray luminosities are compatible with low accretion rates. We encourage theoretical work on globular cluster CVs to try to explain these results, and caution that the low accretion rate interpretation given here is not secure until the combined X-ray and optical luminosities are understood.

Given the relatively high X-ray luminosities of the brightest CVs in 47 Tuc and the observation that about 25% of field CVs are magnetic (Wickramasinghe & Ferrario 2000), is it possible that most of the brighter CVs are DQ Her systems? Solid evidence exists for DQ Her-like behavior in V1 (GHE01a), and the strong resemblance between the spectra of AKO 9 and GK Per suggests that AKO 9 is also a DQ Her system (Knigge et al. 2002b). Unfortunately, these two systems represent just a small fraction of the total CV population in 47 Tuc, and the period versus M_V and F_X/F_{opt} data presented in § 2.2.3 and § 3.2 show that the 47 Tuc CVs are statistically different from DQ Her systems found in the field (field DQ Her's have, on average, significantly brighter optical magnitudes; Fig. 21*b*). This contrasts with the similarity between the L_X distributions of the 47 Tuc CVs and the field DQ Her systems (see Fig. 21*a*).

The L_X and M_V values for the 47 Tuc CVs are consistent with the data presented for NGC 6397 by Cool et al. (1998), Edmonds et al. (1999), and GHE01a. The L_X values of the NGC 6397 CVs are high (like those in 47 Tuc), since four out of nine systems have $L_X > 10^{31.9}$ ergs s^{-1} (GHE01b). Optically the NGC 6397 CVs are faint, despite being expected to have even brighter secondaries than 47 Tuc (because of the low metallicity, [Fe/H] = −1.95; Harris 1996). The absolute magnitudes of the four relatively bright CVs from Cool et al. (1998) and Edmonds et al. (1999) range between 5.95 and 8.81.

Further information about the NGC 6397 CVs is available because good-quality optical spectra have been obtained. Arguments have been made that the CVs in NGC 6397 may be dominated by DQ Her's (Grindlay et al. 1995; Edmonds et al. 1999), based on the observation that three of the four NGC 6397 CVs with measured optical spectra have relatively strong He II 4686 Å lines, like those found in field DQ Her's. Figure 8 of Edmonds et al. (1999) shows an analysis of the absolute magnitudes of the accretion disks [M_V(disk)] for DQ Her systems and the ratio between the continuum levels of Hβ and Hα [C(Hβ)/C(Hα)] for different classes of CV. For field DQ Her systems, linear relationships are found between M_V(disk) and the He II 4686 Å to Hβ equivalent width ratio (He II/Hβ), and a similar relationship is found between [C(Hβ)/C(Hα)] and He II/Hβ (brighter and bluer disks, equivalent to higher accretion rates, correlate with larger He II/Hβ values). The four NGC 6397 CVs discussed in Edmonds et al. (1999) have M_V(disk), [C(Hβ)/C(Hα)], and He II/Hβ values that are consistent with the field DQ Her systems, but intriguingly, the three NGC 6397 CVs with moderate He II/Hβ values are all found in the low accretion rate part of the figure, with low M_V(disk) and low C(Hβ)/C(Hα) values. Therefore, the low accretion rates apparently found for the 47 Tuc CVs, combined with the hints of magnetic behavior in a couple of systems, may be consistent with the NGC 6397 results. Optical spectra of the fainter CVs in NGC 6397 and the large population of CVs in 47 Tuc are needed to test whether they also have relatively strong He II 4686 Å (useful spectra will be difficult to obtain because the CVs are mostly faint and crowded). Searches for rapid WD spin in the optical and X-rays is also needed. Perhaps these observations will identify a new class of low accretion rate, magnetic CVs in globular clusters.

One final possibility worth considering is that somehow the different formation mechanism for globular cluster CVs compared to field CVs is responsible for differences in their respective behavior. To test this hypothesis, we note that CVs in open clusters are much more likely to be formed from primordial binaries than the 47 Tuc CVs. Interestingly, the two CVs discovered in the open cluster NGC 6791 by Kaluzny et al. (1997) are both much bluer (in quiescence) in the V versus $V-I$ CMD than most of the 47 Tuc and NGC 6397 CVs (see Edmonds et al. 1999), suggesting brighter accretion disks and higher accretion rates than the 47 Tuc and NGC 6397 systems. Indeed, one of the NGC 6791 CVs appears to be either a UX UMa or Z Cam system, with a relatively high accretion rate. Only one other CV is

known in an open cluster, a faint AM Her system (EU Cancri) in M67 (Gilliland et al. 1991, see their Fig. 10; Belloni, Verbunt, & Mathieu 1998). Clearly, any two randomly selected CVs from 47 Tuc would not look like the NGC 6791 CVs, but obviously the statistics are very poor. Larger samples of CVs in rich open clusters and low-density globular clusters are needed to see if this effect is significant, or just a statistical anomaly.

4.2. *Active Binaries: Comparison with Field Studies*

We have a total of 29 likely active binaries in 47 Tuc. Twenty-seven of these show statistically significant, mostly periodic, variability, and most of them are found on or slightly above the MS or subgiant ridgeline, except for a handful of red stragglers or red straggler candidates. The total sample of active binaries in 47 Tuc above our X-ray detection threshold will inevitably be larger, since a sensitive variability study was only possible with the GO-8267 data.

A key question is whether the active binaries presented here have properties similar to those of BY Dra's and RS CVn's found in the field. Here we present a brief comparison with the *ROSAT* All-Sky Survey results of Dempsey et al. (1997). Figure 4 of Dempsey et al. (1997) shows that the X-ray luminosities of RS CVn's and BY Dra's are quite different from each other, with median X-ray luminosities of $\sim 1.6 \times 10^{29}$ ergs s^{-1} for the BY Dra's and $\sim 4 \times 10^{30}$ ergs s^{-1} for the RS CVn's, and maximum luminosities of $\sim 2.5 \times 10^{30}$ ergs s^{-1} for the BY Dra's and $\sim 1 \times 10^{32}$ ergs s^{-1} for the RS CVn's. These X-ray luminosities are the quiescent values, as Dempsey et al. (1997) observed flares on all of their targets during their survey and removed data points with enhanced count levels.

The red stragglers ($W3_{opt}$, $W43_{opt}$, and $W72_{opt}$), the red straggler candidates ($W4_{opt}$, $W14_{opt}$, and $W38_{opt}$), and the stars near the MSTO like $W9_{opt}$ and $W75_{opt}$ generally have X-ray luminosities (see GHE01a) that are in good agreement with the Dempsey et al. (1997) data if the primary stars are subgiants and these systems are RS CVn's. The two red stragglers (and possible sub-subgiants) in M67 both have $L_X = 7.3 \times 10^{30}$ ergs s^{-1} (Belloni et al. 1998), in good agreement with the X-ray luminosities of $W3_{opt}$ and $W72_{opt}$. Also, the relatively bright V magnitudes (and in some cases obviously red colors) of the X-ray–bright BY Dra's (Fig. 16*d*) are consistent with the hypothesis that a reasonable number of these objects have at least partially evolved primaries and hence are RS CVn's.

Among the active binaries with optically fainter IDs, the source W47 is probably returning from a flare, and X-ray variability in other sources such as W18, W41, and W94 may also be signs of flares, explaining the relatively high luminosities even though these systems are likely BY Dra's. The luminosities for the optically faint and apparently non–X-ray variable systems like W26, W59, and W66 are obviously more extreme. Some of them could have X-ray variability that is intrinsically quite large, but is not detected because of the faintness of the sources. Another possibility is that they are simply outliers in a large population of objects having a distribution that is similar to those found in the field. AGB01 point out that large numbers of BY Dra's may have been missed in their study due to incompleteness, since the binary frequency determined from the BY Dra sample (with periods that are mostly a few days long) is a factor of 17 smaller than that calculated from the shorter period eclipsing and contact binaries. Assuming that the binary frequency is the same among the BY Dra's in the AGB01 study as it is among the short-period eclipsing and contact binaries, and scaling from the sample of 55 AGB01 binaries with $V > 19$, this would imply a population of about a thousand BY Dra's in 47 Tuc. Since Figure 4 of Dempsey et al. (1997) shows that $\sim$15% of the field BY Dra's have $L_X > 10^{30}$ ergs s^{-1}, we would therefore have a deficit of X-ray detected BY Dra's with $L_X > 10^{30}$ ergs s^{-1}, rather than a surplus. Possible reasons for this deficit are that a reasonable fraction of the binaries with periods longer than about 1–2 days have been destroyed by interactions, or that there is an anticorrelation between L_X and period (see below).

The plot of X-ray color versus V in Figure 22 shows that most of the optically faint active binaries are relatively soft sources, consistent with the expected soft X-ray spectra for these objects in quiescence (Dempsey et al. 1993, 1997). The source W47 is a relatively hard source and is variable, and flares are expected to harden the X-ray spectrum (as noted in Paper I, W64 may show long-term variability).

If the bright active binaries have a substantial fraction of RS CVn's and the faint systems are all BY Dra's, then there may be an anticorrelation between L_X and V (i.e., the optically fainter active binaries being associated with fainter X-ray sources). We found no statistically significant evidence for such an anticorrelation, either with or without the X-ray variables (by contrast, the CVs show weak anticorrelations between L_X and V, especially when AKO 9 is removed from the sample). With a much larger number of (mostly undetected) BY Dra's than RS CVn's, it is much more likely that a few very luminous BY Dra's are detected rather than a few very luminous RS CVn's, possibly explaining the lack of correlation noted above.

In agreement with the trends shown in Figure 17*d*, there is a significant anticorrelation between period and V mag for the active binaries. The linear correlations between period and V are -0.38 and -0.48 when using two different tests (the *kendl1* and *pearsn* subroutines) from Numerical Recipes (Press et al. 1992), with chance probabilities of only 0.4% and 1%. Presumably the main cause of this anticorrelation is that the brighter active binaries contain a number of systems with evolved stars and relatively long periods. However, why have only the short-period BY Dra's (the faint active binaries) been detected in X-rays? According to Dempsey et al. (1997), there is a fairly weak correlation between X-ray flux (F_X) as measured at the Earth and rotation period (P_{rot}) of $F_X \sim P_{rot}^{-0.16 \pm 0.26}$ for BY Dra's (a stronger correlation exists for RS CVn's). Assuming that $L_X = P_{rot}^{-0.16}$ for the active binaries, then the median period of 0.4 days for the faint active binaries (the BY Dra's) and 1.56 days for the faint AGB01 binaries means that L_X would be only 17% lower for the AGB01 binaries. This is probably not a large enough difference to explain the very different period distributions, although a steeper slope (but still remaining within the 1 σ error limit) could easily produce a 30%–40% difference between the X-ray luminosity of the faint active binaries and the faint AGB01 binaries. We also note that the period distribution of the Dempsey et al. (1997) sample is very different from ours, since only 3/29 of the Dempsey et al. (1997) BY Dra's with known periods have periods less than 1 day, but 15/27 of the 47 Tuc active binaries with known periods have periods of less than 1 day (our photometrically selected sample is biased toward short

periods, explaining part of this effect). With this different sample of periods (with a much stronger bias toward short periods), it is not surprising that we find a different F_X/period relationship.

In an important sense our sample of active binaries in 47 Tuc (at fixed metallicity and age) is significantly cleaner than the Dempsey et al. (1997) sample, which contains an inhomogeneous sample of stars with a range of ages and metallicities. Therefore, the examination of trends such as the dependence of F_X on period could be optimally performed with cluster samples (we defer this study to a future publication following analysis of deeper *Chandra* observations obtained in late 2002).

4.3. *Are Some of the Active Binaries MSPs?*

Here we examine the possibility that some of the active binary candidates could be MSPs. Such a population would be very interesting for dynamical reasons (see § 1), and it has a direct impact on the number of MSPs in 47 Tuc estimated from the *Chandra* data. The large range in the estimated number of 47 Tuc MSPs (35–90) given by Grindlay et al. (2002) is dominated by assumptions about the nature of the active binary population (see also § 4.4).

We begin by noting that the eclipsing binary X-ray sources ($W12_{opt}$, $W92_{opt}$, $W137_{opt}$, and $W182_{opt}$) are unlikely to be MSPs (or CVs) because two eclipses would not be expected. Also, the X-ray sources in the AGB01 sample classified as W UMa's ($W41_{opt}$, $W47_{opt}$, and $W163_{opt}$) have periods and colors that obey the Rucinski relationship for such systems (AGB01), therefore making the contact binary explanation a more natural one, although here we do not rule out an MSP explanation.

The radial distributions of the active binaries presented in § 3.1 offer powerful constraints on this issue. There are striking similarities between the radial distributions of the active binaries and the AGB01 binaries (with the active binaries removed) in both the bright and faint samples (see § 3.1 and Fig. 17). The similarity in the bright samples suggests that the bright active binaries are not dominated by MSPs with "normal" MS companions, because then mass segregation would mean that these $\sim$2.15–2.25 $M_\odot$ objects (1.4 $M_\odot$ neutron star +0.75–0.85 $M_\odot$ MS star) should be much more concentrated toward the center of the cluster than the lower mass objects (the radio-detected MSPs and the CVs). There is a chance that some of the bright active binaries could be MSPs with low-mass ($\lesssim$0.2 $M_\odot$) MS star companions that have been heated by X-rays so that they appear optically like MSTO stars or red stragglers, as may be occurring for 6397-A (Ferraro et al. 2001). In principle, the radial distribution of these objects could then mimic those of MSTO binaries; however, this would require a coincidence and would not explain an apparent absence of MSP binaries with MS star companions having masses close to the turnoff value of $\sim$0.85 $M_\odot$. A second possibility is that binary-binary and binary-single star interactions resulting in dynamical kicks may cause the average MSP-MS star binary to be farther away from the center of the cluster than expected for mass segregation of such objects. However, this would require another coincidental similarity between radial distributions. It would also be inconsistent with the difference noted in § 3.1 between the radial distributions of the bright and the faint active binaries. This difference probably would not have been seen if MSPs dominate both the faint and the bright groups, because then the percentage difference in mass between the two groups would have been much smaller (as shown in Fig. 17 the faint active binaries, are unlikely to contain a significant number of MSPs based on their radial distribution).

When these radial distribution results are combined with the evidence that (1) the faint active binaries fall above the MS ridgeline just like the AGB01 sample of binaries (see Paper I), and (2) that the X-ray luminosities are consistent with RS CVn and BY Dra systems (§ 4.2), we conclude that the active binaries are indeed dominated by MS-MS binaries.

Is this finding consistent with the properties of the known MSP population? Of the 16 MSPs with timing positions (Freire et al. 2001), only half of them are binaries and of these only five have companion masses likely to be above the minimum value (0.085 $M_\odot$) for being on the MS (the other three have masses of $\sim$0.02–0.03 $M_\odot$). It is likely that these five MSPs *all* have He WD companions, based on the radio data (Camilo et al. 2000), e.g., 47 Tuc U has an *HST*-identified He WD companion (Edmonds et al. 2001) while a faint, blue star and possible ID has been found for 47 Tuc T, and faint limits can be set in the optical for 47 Tuc H. Only one MS companion was found (47 Tuc W; Edmonds et al. 2002a) in the full sample of 20 MSPs from Camilo et al. (2000). Therefore, if the sample of 16 MSPs is representative of the possibly much larger sample of MSPs (Camilo et al. 2000), then optical companions are rare and MS companions even more so. If a large population of MSPs with MS companions does exist, and we are detecting many of them in X-rays, then the MSPs would have to be intrinsically radio-faint to avoid any of them being detected by Parkes. However, the relatively flat correlation between X-ray and radio luminosity shown by Grindlay et al. (2002) implies that the faintest MSPs in the radio are less faint than X-ray sources.

Given the small number of detections of cluster MSPs with likely nondegenerate companions (two; 47 Tuc W and 6397-A), it is not yet possible to conclude whether such MSPs are generally relatively bright in X-rays but faint in the radio. The MSP 6397-A would have been easily detected by Parkes if it were in 47 Tuc, given the radio luminosity of 5 mJy kpc^2 quoted by D'Amico et al. (2001). The radio luminosities of the 47 Tuc MSPs range between 0.81 and 10.9 mJy kpc^2, with 12 out of 14 of them having radio luminosities less than that of 6397-A. The MSP 47 Tuc W, however, is one of the faintest detected MSPs, and W34, if it is an MSP, is below the detection limit of Camilo et al. (2000). The X-ray luminosities for 6397-A and 47 Tuc W are slightly higher than the most luminous "normal" MSP in 47 Tuc.

Without having a deeper sample of MSPs and detailed radial velocity information for the active binaries, it is very difficult to rule out the possibility that any *individual*, noneclipsing, optical variable has an MSP companion, especially in view of the cases of $W29_{opt}$ and 6397-A (and possibly also $W34_{opt}$). The former object is very crowded optically and was only discovered using difference image analysis (Edmonds et al. 2002a), but was found on close study to have blue colors. Therefore, $W29_{opt}$ would have been classified as a CV instead of an active binary if not for the remarkable period and phase coincidence with 47 Tuc W discovered by Edmonds et al. (2002a), perhaps implying that one or two of the faint CV candidates could be an MSP. None of the active binary candidates show blue

colors, and they also show no hint of the large amplitude variability seen in either $W29_{opt}$ or $W34_{opt}$, despite in some cases having periods that are not much longer than those of $W29_{opt}$ (suggesting similar levels of variability caused by irradiation from an MSP, if present).

One potential source of MSPs masquerading as active binaries are the red stragglers. For example, the companion to the MSP 6397-A was previously identified as a BY Dra by Taylor et al. (2001) on the basis of Hα emission, a CMD position lying above the MS, and optical variability (this star is clearly a red straggler). However, it was subsequently shown by Ferraro et al. (2001) to have an MSP companion based on an accurate radio timing position for the MSP. Naturally, it is possible for a binary system both to be an active binary and to have an MSP companion, since secondaries in short-period binaries like 6397-A are undoubtedly tidally locked and rapidly rotating, and hence may have substantial chromospheric activity (as suggested for 6397-A by Orosz & van Kerkwijk 2003).

Although the 47 Tuc red stragglers and 6397-A have similar optical properties, there are some key differences between their X-ray properties. While 6397-A is a reasonably hard source (as is 47 Tuc W), the two red stragglers W3 and W72 both have very soft X-ray colors, and the two red straggler candidates W4 and W14 also have soft colors (see Figs. 22 and 24). Of the red stragglers, only W43 (in GO-7503) has a hard color. Generally, if most of the active binary candidates are MSPs and are like 47 Tuc W and 6397-A, then they should mostly be hard sources. Yet, of the GO-8267 active binaries with X-ray color determinations from Grindlay et al. (2002), only four (not including $W47_{opt}$) are hard, while nine (not including W4) are soft.

The leading candidates for MSPs hidden within our active binary sample include W43, a faint, moderately hard, variable X-ray source (like 6397-A) with an optical ID that falls in a similar region of the optical CMD to 6397-A, as noted above. No clear optical variability is present, with our limited quality time series. We note that while W43 is clearly harder than the other red stragglers, this could be because of flaring activity, explaining the variability. Both W23 and W64 are moderately hard sources that were not observed to vary during the *Chandra* observation of GHE01a, and are brighter than all of the other active binaries (except W47). However, as explained earlier, W64 may show long-term variability.

The leading candidates for identifications of other 47 Tuc U–like MSPs (not yet detected in the radio) are the weak, soft, nonvariable X-ray sources, with faint, blue, optical companions that do not show long-term variability. These are W82 and W85 (see Figs. 22 and 24), with plausible optical IDs (lying outside the GO-8267 FoV) without obvious long-term variability. They are beyond the faint limit of the GO-7503 data for short-term variability studies. The ID for W70 shows no evidence for periodic variation in our time series and only marginal evidence for nonperiodic variations, but we do not yet have long-term variability information for this object. These sources could be CVs, since AM Her systems, for example, are known to be soft X-ray sources (VBR97). Our high-quality Hα observations with *HST* ACS may help distinguish between these two possibilities, since He WDs should show broad Hα absorption lines, and CVs strong Hα emission lines, as observed for the CVs in NGC 6397 (Grindlay et al. 1995; Cool et al. 1998) and NGC 6752 (Bailyn et al. 1996).

4.4. *Revised Estimate of Total Number of MSPs*

Finally, we examine the soft, faint, apparently nonvariable X-ray sources that have no plausible (optically variable or photometrically unusual) counterparts (see Fig. 24*b*). Grindlay et al. (2002) listed the sources in this category, noting in particular the subset of these sources that fall in the GO-8267 FoV: W4, W5, W6, W24, W28, and W98 (we now add the source W71 to this list). As noted by Grindlay et al. (2002), these sources include the leading candidates to be MSPs. By correcting for the incomplete spatial coverage of the WFPC2 GO-8267 FoV, and for incompleteness in the detection of radio-detected MSPs as soft X-ray sources, Grindlay et al. (2002) estimated the presence of at least 19 MSPs with $L_X \gtrsim 10^{30}$ ergs s^{-1} that do not have radio counterparts with timing positions, in addition to the 16 MSPs with such positions. This estimate obviously increases if some of the active binaries identified with soft sources are instead MSPs, but as argued above, few are expected. Also, the estimate by Grindlay et al. (2002) implicitly assumes that 2/9 of the MSPs have X-ray colors less than 1.0, so a small fraction of misidentified "active binaries" with harder X-ray colors (like W9 or W59) that are really MSPs do not change these statistics.

Based on a study of the optical data, is it reasonable that the seven soft sources just discussed are all MSPs, rather than CVs or active binaries in some cases? First, as already noted, W4 is a candidate red straggler, and W24 may be an RS CVn, and both of them have higher X-ray count levels than the brightest detected MSP (except for the hard X-ray source 47 Tuc W). Also, W98 is located close to several giant stars, so it may also be an RS CVn. To estimate how many active binaries, or perhaps CVs, may have missed detection because of crowding, we have examined the stellar count levels present in the GO-8267 data around the positions of the seven soft sources. Figure 23 shows the mean stellar counts in an annulus (between 0.″9 and 1.″35) around each (1) CV, (2) bright active binary, (3) faint active binary, (4) MSP, (5) unidentified X-ray source, and (6) candidate MSP (the seven sources discussed above). Optical positions are used for (1), (2), (3), and (6), radio positions for (4), and X-ray positions for (5). The median count level for the candidate MSPs is higher than any of these other groups, and is 2.0 times larger than the median count level for the MSPs (the two distributions differ at the 98.8% level using the K-S test). This suggests that some of the seven soft sources are active binaries (or CVs) that have been missed because of crowding. We tentatively classify W4, W24, and W98 as active binaries, based on their proximity to bright stars, and classify the four remaining sources as MSPs. This implies a population of 13 extra MSPs, for a total of 29 MSPs with $L_X > 10^{30}$ ergs s^{-1}.

4.5. *Summary of Optical Identifications*

Incorporating the optical identifications reported here and in Paper I (plus radio/MSP identifications from GHE01a and Grindlay et al. 2002) and just considering the GO-8267 FoV alone (where our high-quality time-series coverage is spatially complete), a significant fraction of the 78 sources are active binaries (34.6%), compared to 19.2%

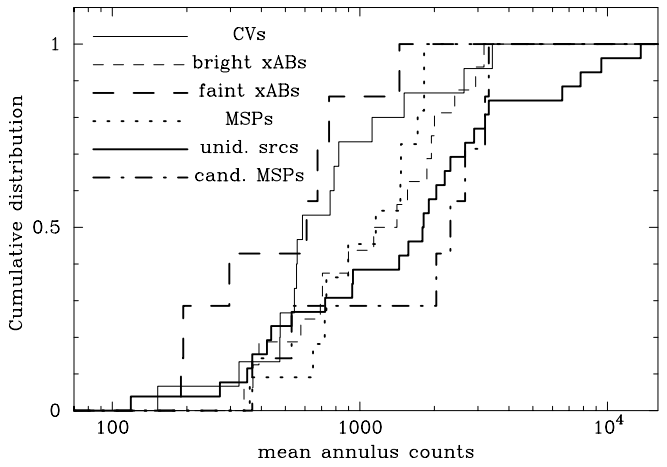

FIG. 23.—Cumulative distribution of mean count values (stellar and background) for annular regions in the GO-8267 V-band image centered on CVs, bright ($V < 19$) active binaries, faint ($V > 19$) active binaries, MSPs, unidentified X-ray sources, and candidate MSPs (soft X-ray sources without optical IDs). The optical positions are used for the CVs and active binaries, the optically corrected radio positions are used for the MSPs (except for 47 Tuc W, where the optical position is used), and the optically corrected X-ray positions are used for the unidentified sources and the candidate MSPs.

for CVs and 9.0% for MSPs, with the source W46/X7 being a qLMXB (1.3%). These sources, where X-ray colors are available, are labeled in the X-ray CMD shown in Figure 24. The remaining 27 (34.6%) sources in the GO-8267 FoV have uncertain identifications, or have no plausible ID. Of these sources, we use the X-ray luminosity and color, or the plausible match-up with bright, blue, or marginally variable stars to tentatively identify W10, W16, W17, W20, W32, W35, W37, and W140 as CVs, and W4, W24, W37, W71, W93, W141, and W168 as active binaries, leaving 13 faint sources that we identify as possible MSPs (see Table 3). This leaves us with final fractions of 42.3% active binaries, 29.5% CVs, and 26.9% MSPs (plus the single qLMXB), although some of the 13 weak X-ray sources could be CVs or active binaries, lowering the MSP number. The CV fraction is very similar to that calculated by GHE01a, but the active binary fraction is significantly higher than the 15% estimated by GHE01a. Correspondingly, the MSP estimate, and the one given in § 4.4, are smaller than the value of ~50 MSPs originally presented for the 108 sources in GHE01a (that estimate was based on incomplete analysis of the optical data).

4.6. *Conclusion and Prospects*

Based on the period/M_V analysis and the M_V distribution presented here, the 47 Tuc CVs appear to have lower accretion rates than field CVs systems found above the period gap. Theoretical work on CV evolution predicts that the fainter, shorter period CVs expected to exist in 47 Tuc (but not observed because of crowding) should have even lower accretion rates than the bright ones that we do observe (see Di Stefano & Rappaport 1994; Townsley & Bildsten 2002). The suggestive evidence for low accretion rates and DQ Her type behavior in CVs in NGC 6397, combined with (1) the evidence for magnetic behavior in a couple of the 47 Tuc CVs (V1 and AKO 9) and (2) the high (DQ Her–like) X-ray luminosities of the 47 Tuc CVs implies that magnetic activity may play an important role in globular cluster CVs. However, more work is needed to understand the unusual M_V and L_X distributions for the CVs in both 47 Tuc and NGC 6397.

Perhaps the most unexpected result, when compared with other clusters, is that the active binaries outnumber the CVs. In NGC 6397, the detected CVs outnumber the active binaries by a factor of ~2–3 (based on deeper *Chandra* data than obtained for 47 Tuc), but significant depletion of the MS binary population in NGC 6397 is likely to have occurred during and after core collapse. In NGC 6752, the detected CVs outnumber the active binaries by a factor of ~4–10, but the NGC 6752 *Chandra* data is not as deep as the 47 Tuc data, and several unidentified soft sources may still be identified with active binaries, given optical data of higher quality.

With this large population of detected active binaries in 47 Tuc, many of them soft sources, we find support for the lower range given by Grindlay et al. (2002) for the number of MSPs in 47 Tuc with $L_X > 10^{30}$ ergs s^{-1} (~30–40). It is possible that a few of the active binaries may really be

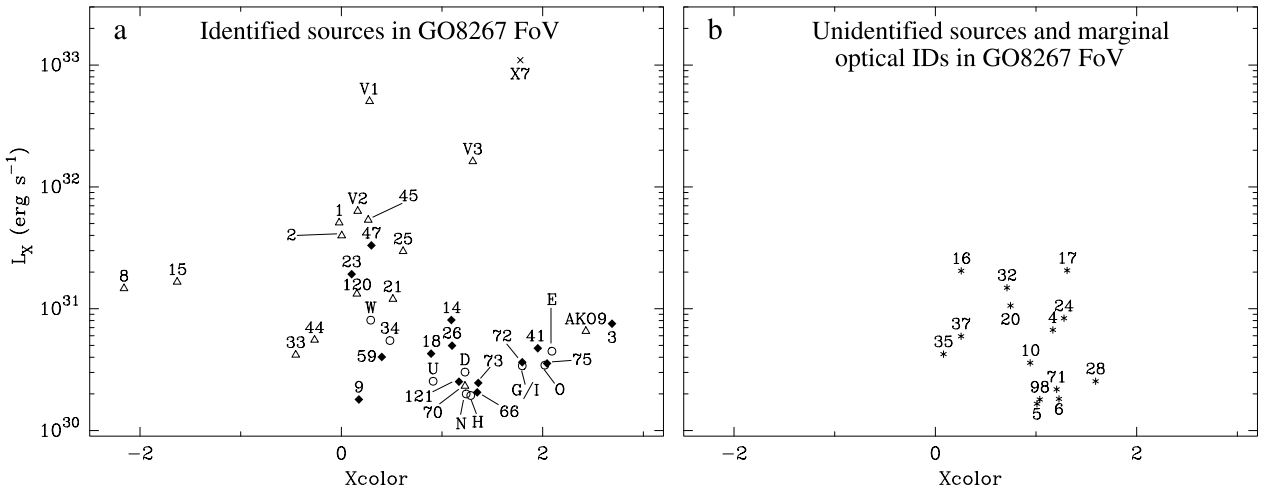

FIG. 24.—X-ray CMD plotting L_X in the 0.5–2.5 keV band versus X-ray color (as defined by GHE01a). (*a*) Optical identifications of CVs, MSPs, and active binaries in the GO-8267 data set, the radio/X-ray identifications of MSPs without optical IDs (47 Tuc D, E, G/I, H, N; Camilo et al. 2000; Freire et al. 2001) and X7 (W46), an X-ray–identified qLMXB (GHE01a; Heinke et al. 2003) without an optical ID (Edmonds et al. 2002b). (*b*) Sources with X-ray colors but lacking optical or radio identifications (some of these have marginal optical IDs).

MSPs, and we continue to search for new objects that are similar to 47 Tuc U or 47 Tuc W, but, given the spatial, photometric, X-ray spectral, and timing information available for the observed active binaries, a large population of MSPs masquerading as active binaries is unlikely. The lower estimated number of MSPs in 47 Tuc means that the ratio between the number of MSPs and the number of CVs is smaller, and closer to the corresponding value found in NGC 6397 by GHE01b.

A comparison of Figures 18 and 19*a* shows that we are sensitive to detection of most classes of CV except for the faintest DNe (SU UMa's), and possibly also double-degenerate systems (where the statistics are poor). There are good prospects for finding at least some of the fainter CV population not yet detected here by using the much deeper X-ray limits set by the 300 ks ACIS-S observation. Although the gains will be limited near cluster center because of X-ray crowding, the faintest CVs should have low-mass companions of $\sim$0.1–0.3 $M_{\odot}$, and with WD masses of $\sim$0.55 $M_{\odot}$ the total system masses should be less than or equal to the MSTO mass. Therefore, many of these objects should be found in relatively uncrowded regions more than 20″–30″ away from the cluster center. Unfortunately, optical identifications will be difficult or impossible for many of these objects because of crowding and the high background levels present in the *HST* images, a penalty for studying objects in this massive, concentrated globular cluster.

The 300 ks follow-up *Chandra* observations will provide much better quality spectral, timing, and positional information, especially for the faintest sources discussed here, and these data should be very useful for distinguishing between MSPs and active binaries. Many new, faint sources will also likely be discovered, dominated by MSPs and active binaries. New radio observations are obviously needed to search for the $\sim$200 undetected MSPs believed to exist in 47 Tuc (Camilo et al. 2000).

We acknowledge comments on the CVs from Brian Warner, and a number of extremely helpful comments from the referee, Christian Knigge. This work was supported in part by STScI grants GO-8267.01-97A (P. D. E. and R. L. G.) and HST-AR-09199.01-A (P. D. E.).

TABLE 3

Chandra Sources with Marginal or No *HST* Counterparts in the GO-8267 Data

Source W	Chip No.	Crowding Level[a]	Plausible ID[b]
20	1	A	CV?
24	1	B	AB?
28	1	A	MSP?
31	1	B	MSP?
32	1	D	CV?
35	1	C	CV?
37	1	B	CV?
39	1	B	47 Tuc O[c]
46	1	B	qLMXB
96	1	A	MSP?[d]
97	1	C	MSP?[d]
98	1	D	AB?
141	1	C	AB?[d]
4	2	D	AB?
5	2	D	MSP?
10	2	D	CV?
13	2	C	47 Tuc N[c]
16	2	D	CV?
17	2	D	CV?
19	2	C	47 Tuc G, I[c]
67	2	C	47 Tuc D[c]
74	2	C	47 Tuc H[c]
91	2	A	MSP?[d]
95	2	B	MSP?[d]
142	2	D	MSP?[d]
168	2	D	AB?[d]
115	3	C	MSP?[d]
6	4	D	MSP?[d]
7	4	D	47 Tuc E[c]
71	4	C	MSP?
93	4	C	AB?[d]
99	4	A	MSP?[d]
140	4	A	CV?[d]

[a] Grade for crowding level: A: Source in uncrowded region; B: Source in moderately crowded region; C: Source in extremely crowded region; D: Source in region affected by saturation.

[b] Plausible source identification based on X-ray spectral information and nearby objects in the optical.

[c] MSP from Camilo et al. 2000.

[d] Source does not formally have an X-ray color, using the criterion of Grindlay et al. 2002.

REFERENCES

Albrow, M. D., Gilliland, R. L., Brown, T. M., Edmonds, P. D., Guhathakurta, P., & Sarajedini, A. 2001, ApJ, 559, 1060 (AGB01)
Augusteijn, T., van der Hooft, F., de Jong, J. A., & van Paradijs, J. 1996, A&A, 311, 889
Bailyn, C. D., Rubenstein, E. P., Slavin, S. D., Cohn, H., Lugger, P., Cool, A. M., & Grindlay, J. E. 1996, ApJ, 473, L31
Belloni, T., Verbunt, F., & Mathieu, R. D. 1998, A&A, 339, 431
Camilo, F., Lorimer, D. R., Freire, P., Lyne, A. G., & Manchester, R. N. 2000, ApJ, 535, 975
Cool, A. M., Grindlay, J. E., Cohn, H. N., Lugger, P. M., & Bailyn, C. D. 1998, ApJ, 508, L75
D'Amico, N., Possenti, A., Manchester, R. N., Sarkissian, J., Lyne, A. G., & Camilo, F. 2001, ApJ, 561, L89
Dempsey, R. C., Linsky, J. L., Fleming, T. A., & Schmitt, J. H. M. M. 1997, ApJ, 478, 358
Dempsey, R. C., Linsky, J. L., Schmitt, J. H. M. M., & Fleming, T. A. 1993, ApJ, 413, 333
Di Stefano, R., & Rappaport, S. 1994, ApJ, 423, 274
Edmonds, P. D., Gilliland, R. L., Camilo, F., Heinke, C. O., & Grindlay, J. E. 2002a, ApJ, 579, 741
Edmonds, P. D., Gilliland, R. L., Guhathakurta, P., Petro, L. D., Saha, A., & Shara, M. M. 1996, ApJ, 468, 241
Edmonds, P. D., Gilliland, R. L., Heinke, C. O., & Grindlay, J. E. 2003, ApJ, 596, 1177 (Paper I)
Edmonds, P. D., Gilliland, R. L., Heinke, C. O., Grindlay, J. E., & Camilo, F. 2001, ApJ, 557, L57
Edmonds, P. D., Grindlay, J. E., Cool, A., Cohn, H., Lugger, P., & Bailyn, C. 1999, ApJ, 516, 250
Edmonds, P. D., Heinke, C. O., Grindlay, J. E., & Gilliland, R. L. 2002b, ApJ, 564, L17
Ferraro, F. R., Possenti, A., D'Amico, N., & Sabbi, E. 2001, ApJ, 561, L93
Freire, P. C., Camilo, F., Lorimer, D. R., Lyne, A. G., Manchester, R. N., & D'Amico, N. 2001, MNRAS, 326, 901
Gilliland, R. L., Bono, G., Edmonds, P. D., Caputo, F., Cassisi, S., Petro, L. D., Saha, A., & Shara, M. M. 1998, ApJ, 507, 818
Gilliland, R. L., et al. 1991, AJ, 101, 541
———. 2000, ApJ, 545, L47
Grindlay, J. E., Camilo, F., Heinke, C. O., Edmonds, P. D., Cohn, H., & Lugger, P. 2002, ApJ, 581, 470
Grindlay, J. E., Cool, A. M., Callanan, P. J., Bailyn, C. D., Cohn, H. N., & Lugger, P. M. 1995, ApJ, 455, L47
Grindlay, J. E., Heinke, C. O., Edmonds, P. D., & Murray, S. 2001a, Science, 292, 2290 (GHE01a)
Grindlay, J. E., Heinke, C. O., Edmonds, P. D., Murray, S. S., & Cool, A. M. 2001b, ApJ, 563, L53 (GHE01b)
Harris, W. E. 1996, AJ, 112, 1487
Heinke, C. O., Edmonds, P. D., & Grindlay, J. E. 2001, ApJ, 562, 363

Heinke, C. O., Grindlay, J. E., Lloyd, D., & Edmonds, P. D. 2003, ApJ, in press
Hessman, F. V., Gänsicke, B. T., & Mattei, J. A. 2000, A&A, 361, 952
Hut, P., et al. 1992, PASP, 104, 981
Kaluzny, J., Stanek, K. Z., Garnavich, P. M., & Challis, P. 1997, ApJ, 491, 153
Kaluzny, J., & Thompson, I. B. 2002, peprint (astro-ph/0210626)
Knigge, C., Zurek, D. R., Shara, M. M., & Long, K. S. 2002a, ApJ, 579, 752
Knigge, C., Zurek, D. R., Shara, M. M., Long, K. S., & Gilliland, R. L. 2002b, in ASP Conf. Ser. 263, Stellar Collisions, Mergers, and their Consequences, ed. M. M. Shara (San Francisco: ASP)
Mathieu, R. D., van den Berg, M., Torres, G., Latham, D., Verbunt, F., & Stassun, K. 2002, preprint (astro-ph/0209568)
Neill, J. D., Shara, M. M., Caulet, A., & Buckley, D. A. H. 2002, AJ, 123, 3298
Orosz, J. A., & van Kerkwijk, M. H. 2003, A&A, 397, 237
Press, W. H., Teukolsky, S. A., Vetterling, W. T., & Flannery, B. P. 1992, Numerical recipes in C (2d Ed.; Cambridge: Cambridge Univ. Press)
Richman, H. R. 1996, ApJ, 462, 404
Ritter, H., & Kolb, U. 1998, A&AS, 129, 83
Russell, H. N. 1945, ApJ, 102, 1
Shara, M. M., Bergeron, L. E., Gilliland, R. L., Saha, A., & Petro, L. 1996, ApJ, 471, 804
Sills, A., Bailyn, C. D., Edmonds, P. D., & Gilliland, R. L. 2000, ApJ, 535, 298
Stehle, R., Kolb, U., & Ritter, H. 1997, A&A, 320, 136
Taylor, J. M., Grindlay, J. E., Edmonds, P. D., & Cool, A. M. 2001, ApJ, 553, L169
Townsley, D. M., & Bildsten, L. 2002, ApJ, 565, L35
Verbunt, F., Bunk, W. H., Ritter, H., & Pfeffermann, E. 1997, A&A, 327, 602 (VBR97)
Verbunt, F., & Hasinger, G. 1998, A&A, 336, 895
Warner, B. 1995, Cataclysmic Variable Stars (Cambridge: Cambridge Univ. Press)
Wickramasinghe, D. T., & Ferrario, L. 2000, PASP, 112, 873
Yi, I. 1994, ApJ, 422, 289
Zoccali, M., et al. 2001, ApJ, 553, 733